

Research Article

Finite Difference Method for Infection Model of HPV with Cervical Cancer under Caputo Operator

Bushra Bajjah ^{1,2} and Mahmut Modanli ²

¹*Tamar University, Faculty of Applied Sciences, Department of Mathematics, Dhamar, Yemen*

²*Harran University, Faculty of Arts and Sciences, Department of Mathematics, Şanlıurfa 63300, Türkiye*

Correspondence should be addressed to Bushra Bajjah; bushra.bajjah@tu.edu.ye

Received 8 August 2023; Revised 8 January 2024; Accepted 16 April 2024; Published 15 May 2024

Academic Editor: Francisco R. Villatoro

Copyright © 2024 Bushra Bajjah and Mahmut Modanli. This is an open access article distributed under the Creative Commons Attribution License, which permits unrestricted use, distribution, and reproduction in any medium, provided the original work is properly cited.

In this paper, a fractional model in the Caputo sense is used to characterize the dynamics of HPV with cervical cancer. Generalized mean value theorem has been used to examine whether the infection model has a unique positive solution. The model has two equilibrium points: the disease-free point and the endemic point. The examination of the system's local and global stability is provided in terms of the basic reproductive number (\mathcal{R}_{p_0}). The global stability analysis has been carried out using an appropriate Lyapunov function and the LaSalle invariant principle. The results demonstrate that in the infection model, if $\mathcal{R}_{p_0} < 1$, then the solution converges to the disease-free equilibrium, which is both locally and globally asymptotically stable. Whilst $\mathcal{R}_{p_0} > 1$, the endemic equilibrium is considered to exist. Simulations are implemented via a finite difference method with Grünwald-Letnikov discretization approach for Caputo derivative operator to define how changes in parameters impact the dynamic behavior of the system using Matlab.

1. Introduction

The most prevalent sexually transmitted infectious agent in both sexes worldwide is the human papillomavirus (HPV), which gets its name from warts (papillomas) [1]. HPVs are small DNA viruses that attack the cutaneous or mucosal epithelium [2]. There are more than 170 different varieties of HPV that have been found and categorized, and more than 40 of these viruses are the most widespread sexually transmitted ailment in the world [3]. One of the main causes of anal cancer, cervical cancer (CC), and other cancers is HPV. Each year, more than 400000 new cases are reported worldwide, and more than 300 women's lives were lost to HPV-related causes in just 2018 [4]. Based on the severity of clinical manifestations, genital HPV types are divided into high-risk as subtypes (16, 18, 31, 33, 35, 39, 45, 51, 52, 56, 58, 59, 68, 73, 82) associated with premalignant and malignant cervical, penile, vulvar, vaginal, anal, head, and neck cancers;

and low-risk such as subtypes (6, 11, 42, 44, 51, 53, 83) that cause warts or benign, highly proliferative lesions on the genitals [5].

It has been determined that a high-risk HPV DNA sequence, notably HPV 16 and 18, which are present in around 70% of invasive cancers, is present in approximately 99.8% of CC [6]. The World Health Organization (WHO) developed a global strategy to hasten the elimination of CC by 2020 and urged for its eradication as a public health problem in 2018 [7]. It classes as the fourth most frequent malignancy in women, with an anticipated 604,000 new cases and 342,000 fatalities worldwide in 2020 [8].

Infectious disease modeling has drawn a lot of interest recently in an effort to find cures for the diseases and calamities that have beset humanity [9]. A system of equations with state variables and parameters is used in the mathematical model to show the interconnectedness of theories and observations and to investigate approximations and the

effects of the parameters as well as anticipate the behavior of the problem over a particular period of time [10] and provide policymakers in public health with information on how to carry out efficient infection control interventions [11]. The fundamental quantities like as birth rates, transmission rates, recovery rates, and mortality rates are expressed by parameters, which are constants incorporated into the equations [12]. Fractional-order differential equation models are utilized as an alternative approach since integer-order differential equations can't adequately describe experimental and field measurement data. More degrees of freedom and the inclusion of memory effects are advantages of fractional-order differential equation systems over conventional differential equation systems. To put it another way, they offer a useful tool for expressing memory and hereditary aspects that were not included in the classical integer-order system [13]. A variety of fractional operator types are introduced to obtain a deeper understanding of the behavior of the models. These operators have various advantages and disadvantages over each other, such as Riemann-Liouville, Caputo, Caputo-Fabrizio, Hadamard, Katugampola, Atangana-Baleanu, and many more [14]. Furthermore, unlike conventional integer-order derivatives, fractional-order derivatives such as the Caputo-Fabrizio derivative; have a non-singular kernel property. This property makes it very evident that when modeling realistically, the model's future state depends on both its current and past states [15]. Moreover, the fractional-order explains some characteristics of the dynamical system for the entire time and provides a complete description of the system that covers the entire process space, whereas the classical integer-order derivative addresses certain dynamic characteristics at a specific time [16]. The realization that the majority of challenging dynamical systems are found to be non-singular is recently credited with the enormous increase in the treatment of dynamical systems with fractional-order derivatives. Additionally, they have a lengthy memory, which allows them to provide overall systems effectively [17]. The Mittag-Leffler function and the exponential decay functions, respectively, are used as the kernels of non-singular derivatives like the Atangana-Baleanu and Caputo-Fabrizio fractional derivatives, whilst the power function is used as the kernel of singular derivatives like Caputo [18]. It's hardly surprising that a lot of models have been researched using fractional-order derivatives given their enormous and wealthy properties. As an illustration, Paul et al. [19] created and studied the SEIR model using fractional-order Caputo derivatives, considering two time-lags: the time required to heal sick individuals and the temporary immune period. Jahanshahi et al. [20] investigated a fractional-order SIRD model in Caputo's sense with time-dependent memory indexes to include the multi-fractional properties of COVID-19. Caputo fractional derivatives were used by Naik et al. [21] to analyze a fractional-order model for the HIV epidemic's propagation with optimal control. Chu et al. [22] examined the Holling type II form, a vector-host infectious illness compartmental model with nonlinear saturated incidence and therapy functions. Firstly, the model is formulated mathematically as a nonlinear classical integer-order

deferential system. To more accurately represent the dynamics of the disease, the subsequently extended the model to the fractional order by utilizing the well-known Caputo-Fabrizio operator with an exponential decay kernel. Atangana-Baleanu Caputo operator has been used in [9] to examine the diabetes mellitus fractional-order model. Qureshi [14] suggested using Caputo fractional-order operator to create a novel epidemiological system for the measles pandemic. In [23], a model of the dynamics of HIV and malaria transmission with optimal control was created using a Caputo fractional derivative. Owolabi and Edson [24] used the Caputo operator and fixed point theory to model and investigate tuberculosis (TB). Utilizing the Caputo derivative, the dynamical analysis of a fractional-order time-delay glucose-insulin model was carried out in [25]. The researcher in [26] studied a variable-order fractional mathematical model driven by Lévy noise describing the model of the Omicron virus using the concept of Caputo derivative. For additional information on several different forms of fractional derivatives, see reference [27] as well as the references cited therein.

Many researchers created mathematical models to represent the ailment's dynamics, which helped them to propose ailment control strategies and characterize the dynamics of co-infection with other infectious ailments. The dynamics of HPV and CC (HPV-CC) with preventative strategies including screening, vaccination, and re-vaccination were described using an ordinary differential equation model developed in [28]. Chakraborty et al. [29] developed a mathematical model to analyze how vaccination affects the dynamics of HPV infection prevention and looked into the viability of a vaccination strategy, illustrating analytically and numerically how vaccination can ensure a predictable preventive policy against disease transmission among sexually active individuals who are more likely to develop CC from high-risk and low-high-risk papillomavirus strains, whilst the same mathematical model in the fractional-order with Atangana-Baleanu derivatives was studied, and numerical solutions were obtained using the Adams-Bashforth-Moulton method by [30]. The most crucial epidemiological aspects of HPV infection and related cancers were incorporated into a two-sex deterministic mathematical model that was developed by the researchers in [31]. The model included catch-up vaccination for adults and school-based vaccine administration for teenagers to evaluate the population-level effects of HPV immunization programs. The center manifold theorem, normal forms theory, and the next-generation operator were all used to thoroughly study the model's dynamics. For several conceivable scenarios, they created an optimal control problem to identify the best HPV vaccination deployment method. They proved that there are optimum control issue solutions and used Pontryagin's Maximum Principle to describe the prerequisites for optimal control solutions. Akimenko and Fajar studied the stability of the age-structured model of CC cells and HPV dynamics [32]. In [33], the author has researched how antiviral treatments affect the spread of cervical cancer. The model includes two pharmacological therapies. The function of the first one is to prevent new

infections, while the second's function is to prevent viral replication. The numerical outcomes have demonstrated the role of the provided medication in regulating HPV infection and cancer cell growth rate. In [34], the mathematical model for the dynamics of HPV transmission in-host in the presence of an immune response represented by Cytotoxic T-lymphocytes cells has been studied; the model presented taking into account the effects of latent HPV infections, and the dynamics of the model were successfully analyzed. A new mathematical model of CC based on the age-structured of cells at the tissue level has been put out by researchers in [35]. Goshu and Alebachew [36] created a mathematical model for the spread of CC transmission disease in the presence of vaccination and therapy. Omame et al. [37] created and presented a coinfection classical integer-order model for syphilis and HPV with cost-effectiveness analysis and optimal control. While the fractional-order in the Caputo–Fabrizio sense of the coinfection model for HPV and Syphilis is investigated using the nonsingular kernel derivative [38]. HPV and *Chlamydia trachomatis* coinfection mathematical model with cost-effectiveness optimal control analysis has been formulated and examined. It has been investigated how HPV screening, *Chlamydia trachomatis* therapy, and both diseases' preventive measures affect the management of their coinfections, the consequent prevention of malignancies, and pelvic inflammatory disease [39], and Nwajeri et al. [40] researched the fractional-order with Caputo derivatives of the codynamics model for HPV and *Chlamydia trachomatis*, and created the numerical simulations utilizing the fractional predictor-corrector method. In [41] they developed an optimal control strategy for the HPV-Herpes Simplex Virus type 2 codynamics model that minimizes the cost of implementing controls while also minimizing the number of infectious individuals over the intervention interval. The Runge-Kutta forward-backward sweep numerical approximation method was used to implement the optimal control systems.

In light of these accomplishments, we are inspired to investigate the HPV-CC model in this study with the Caputo fractional-order operator, which is best appropriate for

modeling biological and physical facts. The motivation to continue our investigation with the Caputo derivative which is a modification of the Riemann–Liouville definition is that this type of fractional operator has advantages concerning other present derivatives; the Caputo derivative of a constant function yields zero, which is usual in mathematics. The Caputo operator first solves an ordinary differential equation, then it takes a fractional integral to get the desired fractional derivative order. More crucially, Caputo's fractional differential equation allows the use of local initial conditions to be included in the derivation of the model, and finally, the inclusion of the memory effect on the Caputo derivative.

The purpose of this study is to investigate the dynamics of the fractional-order of the HPV-CC model, using the Caputo derivative. The organization of the paper is as follows: Some essential definitions and fractional calculus properties are given in Section 2. The fractional HPV-CC model is introduced in Section 3, along with proof of the solutions' existence and uniqueness. In Section 4, it is shown that the suggested model is locally stable at the disease-free and endemic equilibrium points. The global stability of the suggested model at the disease-free and endemic equilibrium points is examined in Section 5. In Section 6, we construct a finite difference scheme for the suggested model and show that it maintains the boundedness and positivity of the solutions to the investigated model; here, we will discuss the asymptotic stability of this scheme. To demonstrate the applicability and effectiveness of the finite difference method, some numerical simulations for the suggested model are shown in Section 7, and the final Section is devoted to the conclusion.

2. Preliminary Concepts

Some basic results pertaining to fractional calculus are presented in this section.

Definition 1. Laplace transform of the function $g(x)$ is defined by the following improper integral,

$$\mathcal{L}(g(x)) := G(s) := \int_0^\infty e^{-sx} g(x) dx := \lim_{m \rightarrow \infty} \int_0^m e^{-sx} g(x) dx, \quad s \in \mathbb{C}, \Re(s) > 0. \quad (1)$$

Definition 2. MittagLeffler function is defined as

$$E_\omega(y) = \sum_{n=0}^\infty \frac{y^n}{\Gamma(\omega n + 1)}, \quad y \in \mathbb{C}, \Re(\omega) > 0. \quad (2)$$

Definition 3. Mittag-Leffler function of two parameters (generalization of Mittag-Leffler function) is given by

$$E_{\omega,\nu}(y) = \sum_{n=0}^\infty \frac{y^n}{\Gamma(\omega n + \nu)}, \quad y, \nu \in \mathbb{C}, \Re(\omega) > 0. \quad (3)$$

Lemma 4. For $c \in \mathbb{R}$ and $\omega, \nu > 0$, we acquire

$$\mathcal{L}(y^{\nu-1} E_{\omega,\nu}(cy^\omega)) = \frac{s^{\omega-\nu}}{s^\omega - c}. \quad (4)$$

Definition 5. Riemann-Liouville fractional integral of order $\beta > 0, a \geq 0$ of a function $g: \mathbb{R}_{\geq 0} \rightarrow \mathbb{R}$ is defined by

$$I_a^\beta g(x) := \frac{1}{\Gamma(\beta)} \int_a^x (x - \xi)^{\beta-1} g(\xi) d\xi, \quad x > a. \quad (5)$$

Definition 6. Caputo fractional derivative of order $\beta > 0, a \geq 0$ for a function $g(x)$ where $g \in C^m([a, \infty), \mathbb{R})$ and $m = [\beta]$ is given by

$$\begin{aligned} {}^c D_x^\beta g(x) &:= I_a^{m-\beta} D^m g(x) \\ &:= \frac{1}{\Gamma(m-\beta)} \int_a^x (x-\xi)^{(m-\beta-1)} \frac{d^m}{d\xi^m} g(\xi) d\xi, \quad m-1 < \beta < m. \end{aligned} \tag{6}$$

Definition 7. Caputo fractional derivative on the half axis $\mathbb{R}_{\geq 0}$ of order $\beta > 0$ of a function $g(x) \in C^m([0, \infty), \mathbb{R})$ and $m = [\beta]$ is defined as follows

$${}^c D_t^\beta g(x) := \frac{1}{\Gamma(m-\beta)} \int_0^x (x-\xi)^{(m-\beta-1)} \frac{d^m}{d\xi^m} g(\xi) d\xi, \quad x > 0, m-1 < \beta < m. \tag{7}$$

When $0 < \beta < 1$, (7) takes the the following form

$${}^c D_x^\beta g(x) := \frac{1}{\Gamma(1-\beta)} \int_0^x (x-\xi)^{(-\beta)} g'(\xi) d\xi, \quad x > 0. \tag{8}$$

3. HPV-CC Model Formulation

This work examines a modified version of the classical integer-order HPV-CC model that was previously examined in [42]. The model's classes have been defined as follows: The total individual population who are sexually active at time t , denoted by $(N_p(t))$, is divided into five compartments: susceptible individuals ($S(t)$), individuals exposed to HPV ($E_p(t)$), infectious individuals showing no symptoms of HPV ($A_p(t)$), infectious individuals showing symptoms of HPV ($I_p(t)$), and individuals infected with CC ($C(t)$). Thus, $N_p(t) = S(t) + E_p(t) + A_p(t) + I_p(t) + C(t)$.

Susceptible individuals acquire HPV infection with an infection force of

$$\lambda_p = \frac{\mathcal{B}_p q_p (r_3 A_p + r_4 I_p)}{N_p}, \tag{9}$$

where, \mathcal{B}_p represents the rate of HPV infection transmission, q_p represents effective contact rate, r_3 , and r_4 represent the relative infectiousness of A_p and I_p respectively with ($r_3 < r_4$).

With probability q where $0 < q < 1$, individuals in class E_p develop to individuals in class I_p , individuals in class E_p

develop to individuals in class A_p with probability $(1 - q)$. After experiencing an HPV symptom, individuals in class A_p proceed to individuals in class C with a rate w_3 . Individuals in class I_p compartments may have CC with the rate of development α_3 . Based on the formulations and presumptions mentioned above, the HPV-CC model takes the following form (associated biological parameters of the model are shown in Table 1) [42]:

$$\left\{ \begin{aligned} \frac{dS(t)}{dt} &= \pi - (\lambda_p + \mu)S, \\ \frac{dE_p(t)}{dt} &= \lambda_p S - (\eta + \mu)E_p, \\ \frac{dA_p(t)}{dt} &= (1 - q)\eta E_p - (w_3 + \mu)A_p, \\ \frac{dI_p(t)}{dt} &= q\eta E_p - (\alpha_3 + \mu)I_p, \\ \frac{dC(t)}{dt} &= \alpha_3 I_p + w_3 A_p - \mu C, \end{aligned} \right. \tag{10}$$

With the following non-negative initial conditions,

$$S(0) = S_0, E_p(0) = E_{p0}, A_p(0) = A_{p0}, I_p(0) = I_{p0}, C(0) = C_0. \tag{11}$$

The reason for examining the fractional-order case is the noteworthy uniqueness of these fractional-order systems with hereditary qualities and non-local features (memory)

that have not been observed with the integer-order differential operators commonly found in biology. Additionally, mistakes resulting from overlooked parameters can be

TABLE 1: Biological description of parameters used in HPV-CC model (10).

Parameter	Description
π	Recruitment rate of individuals
\mathcal{B}_p	Transmission rate
q_p	Contact rate
r_3	Relative infectiousness of asymptomatic individuals
r_4	Relative infectiousness of symptomatic individuals
q	Probability of exposed individuals developing into symptomatic individuals
w_3	Progression rate from asymptomatic individuals to those having cervical cancer individuals
α_3	Progression rate from symptomatic individuals to those having cervical cancer individuals
μ	Natural mortality rate of individuals
η	Mortality rate of the exposed individuals

minimized by modeling real-life processes with fractional-order differential equations [21]. As a result, our suggested fractional-order model for HPV-CC using the Caputo derivatives is:

$$\begin{cases} {}^c_0D_t^\beta S(t) = \pi - (\lambda_p + \mu)S, \\ {}^c_0D_t^\beta E_p(t) = \lambda_p S - (\eta + \mu)E_p, \\ {}^c_0D_t^\beta A_p(t) = (1 - q)\eta E_p - (w_3 + \mu)A_p, \\ {}^c_0D_t^\beta I_p(t) = q\eta E_p - (\alpha_3 + \mu)I_p, \\ {}^c_0D_t^\beta C(t) = \alpha_3 I_p + w_3 A_p - \mu C. \end{cases} \quad (12)$$

Subject to the initial conditions (11), where $\beta \in (0, 1]$, $N_p(t) = S(t) + E_p(t) + A_p(t) + I_p(t) + C(t)$, and $(S(t), E_p(t), A_p(t), I_p(t), C(t)) \in \mathbb{R}_{\geq 0}^5$. If $\beta = 1$ then Model (12) reduces to Model (10).

Biological parameters in Model (12) have been modified to make sure that the left and right-hand sides of the model have the same dimension ($t^{-\beta}$) as follows (the schematic diagram of Model (13) is shown in Figure 1):

$$\begin{cases} {}^c_0D_t^\beta S(t) = \pi^\beta - (\lambda_p^\beta + \mu^\beta)S, \\ {}^c_0D_t^\beta E_p(t) = \lambda_p^\beta S - (\eta^\beta + \mu^\beta)E_p, \\ {}^c_0D_t^\beta A_p(t) = (1 - q)\eta^\beta E_p - (w_3^\beta + \mu^\beta)A_p, \\ {}^c_0D_t^\beta I_p(t) = q\eta^\beta E_p - (\alpha_3^\beta + \mu^\beta)I_p, \\ {}^c_0D_t^\beta C(t) = \alpha_3^\beta I_p + w_3^\beta A_p - \mu^\beta C, \end{cases} \quad (13)$$

here, $\lambda_p^\beta = (\mathcal{B}_p q_p (r_3^\beta A_p + r_4^\beta I_p) / N_p)$.

3.1. Existence and Uniqueness of Non-Negative Solutions. Consider the following initial value problem of autonomous nonlinear Caputo fractional-order derivative system

$${}^c_0D_t^\beta \mathbf{g}(t) = \mathbf{f}(\mathbf{g}(t)), \beta \in (0, 1), \quad \forall t \geq 0, \quad (14)$$

combined with the initial condition

$$\mathbf{g}(0) = \mathbf{g}_0 \geq 0, \quad (15)$$

where $\mathbf{g}_0 \in \mathbb{R}^n$ and the function $\mathbf{f}(\mathbf{g}(t)): \mathbb{R}^n \rightarrow \mathbb{R}^n, n \geq 1$ is called vector field.

Theorem 8 (see [43]). *Suppose that $\mathbf{f}(\mathbf{g}(t))$ attains the following conditions:*

- (i) $\mathbf{f}(\mathbf{g}(t))$ and $(\partial \mathbf{f} / \partial \mathbf{g})(\mathbf{g}(t))$ are continuous,
- (ii) $\|\mathbf{f}(\mathbf{g}(t))\| \leq \iota + j \|\mathbf{g}(t)\|, \iota, j \in (0, +\infty)$,

For almost each $t \in \mathbb{R}$ and every $\mathbf{g} \in \mathbb{R}^n$. Then, the solution of (14) and (15) is not only existent but also unique on $[0, +\infty)$.

Lemma 9 (see [44]). *(Generalized mean value theorem) Assume that $\mathbf{g}(t)$ and ${}^c_0D_t^\beta \mathbf{g}(t)$ with $\beta \in (0, 1)$ are continuous for each $t \in [0, b]$ and $t \in (0, b)$ respectively, then, one has*

$$\mathbf{g}(t) = \mathbf{g}(0) + \frac{1}{\Gamma(\beta)} ({}^c_0D_t^\beta \mathbf{g})(\gamma) t^\beta, \gamma \in [0, t], \forall t \in (0, b]. \quad (16)$$

Lemma 10 (see [45]). *Assume that $\mathbf{g}(t) \in C[0, b]$ and ${}^c_0D_t^\beta \mathbf{g}(t) \in (0, b]$ with $\beta \in (0, 1)$.*

- (i) If ${}^c_0D_t^\beta \mathbf{g}(t) \geq 0, \forall t \in (0, b)$. then $\mathbf{g}(t)$ is increasing $\forall t \in [0, b]$.
- (ii) If ${}^c_0D_t^\beta \mathbf{g}(t) \leq 0, \forall t \in (0, b)$. then $\mathbf{g}(t)$ is decreasing $\forall t \in [0, b]$.

Theorem 11. *For any initial condition fulfilling (15), System (14) has a unique solution $\mathbf{g}(t) = [g_1(t), g_2(t), \dots, g_n(t)]^T$ on $t \geq 0$. Additionally, $\mathbf{g}(t)$ is still in $\mathbb{R}_{\geq 0}^n$ and bounded.*

Theorem 12. *Model (13) has a unique solution on $[0, +\infty)$ for positive initial conditions (11) and this solution is still in $\mathbb{R}_{\geq 0}^5$ for every $t \geq 0$. Furthermore, $N_p(t) \leq \pi^\beta / \mu^\beta$.*

Proof. Let us reformulate Model (13) in the form of Caputo fractional derivative system of order $\beta \in (0, 1]$, as follows

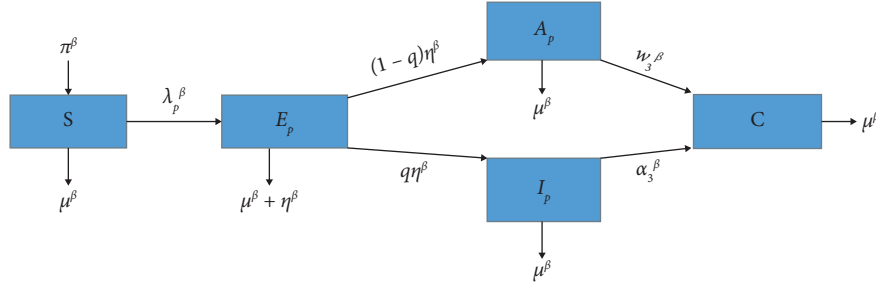


FIGURE 1: Schematic diagram of HPV-CC model (13).

$${}^c_0D_t^\beta \mathbf{g}(t) = \mathbf{f}(\mathbf{g}(t)) = \zeta + \mathbf{B}_1 \mathbf{g}(t) + \frac{S}{N_p} \mathbf{B}_2 \mathbf{g}(t), \forall t \geq 0, \text{ with } \mathbf{g}(0) = \mathbf{g}_0 \in \mathbb{R}_{\geq 0}^5, \quad (17)$$

where $\mathbf{f}: \mathbb{R}^5 \rightarrow \mathbb{R}^5$, $\mathbf{g}(t) = (S(t), E_p(t), A_p(t), I_p(t), C(t))^T$, $\zeta = (\pi^\beta, 0, 0, 0, 0)^T$,

$$\mathbf{B}_1 = \begin{pmatrix} -\mu^\beta & 0 & 0 & 0 & 0 \\ 0 & -\dot{a} & 0 & 0 & 0 \\ 0 & (1-q)\eta^\beta & -\dot{d} & 0 & 0 \\ 0 & q\eta^\beta & 0 & -\dot{e} & 0 \\ 0 & 0 & w_3^\beta & \alpha_3^\beta & -\mu^\beta \end{pmatrix}, \quad (18)$$

$$\mathbf{B}_2 = \begin{pmatrix} 0 & 0 & -\mathcal{B}_p q_p r_3^\beta & -\mathcal{B}_p q_p r_4^\beta & 0 \\ 0 & 0 & \mathcal{B}_p q_p r_3^\beta & \mathcal{B}_p q_p r_4^\beta & 0 \\ 0 & 0 & 0 & 0 & 0 \\ 0 & 0 & 0 & 0 & 0 \\ 0 & 0 & 0 & 0 & 0 \end{pmatrix}.$$

Here $\dot{a} = \eta^\beta + \mu^\beta$, $\dot{d} = w_3^\beta + \mu^\beta$, and $\dot{e} = \alpha_3^\beta + \mu^\beta$.

It is clear that vector function $\mathbf{g}(t)$ satisfies the first condition of Theorem 11. The second one needs to be proven. From System (17), we get, $\|{}^c_0D_t^\beta \mathbf{g}(t)\| \leq \|\zeta\| + (\|\mathbf{B}_1\| + \|(S/N_p)\| \|\mathbf{B}_2\|) \|\mathbf{g}(t)\|$. Hence, the second condition of Theorem 11 is proven. Next, we need to prove that this solution is nonnegative. From (13), we have ${}^c_0D_t^\beta S(t)|_{S=0} = \pi^\beta > 0$, ${}^c_0D_t^\beta E_p(t)|_{E_p=0} = \lambda_p^\beta S \geq 0$ for all $S > 0$, $I_p, A_p, E_p, C \geq 0$, ${}^c_0D_t^\beta A_p(t)|_{A_p=0} = (1-q)\eta^\beta E_p \geq 0$ for all $E_p \geq 0$, ${}^c_0D_t^\beta I_p(t)|_{I_p=0} = q\eta^\beta E_p \geq 0$ for all $E_p \geq 0$, ${}^c_0D_t^\beta C(t)|_{C=0} = \alpha_3^\beta I_p + w_3^\beta A_p \geq 0$ for all $I_p, A_p \geq 0$.

We conclude that the solution of Model (13) will remain in $\mathbb{R}_{\geq 0}^5$ based on Lemmas 9 and 10.

Finally, we demonstrate that the solution is bounded. Adding Model's (13), results in

$${}^c_0D_t^\beta N_p(t) = \pi^\beta - \mu^\beta N_p(t). \quad (19)$$

Taking Laplace transform in (19) into account, we get $\mathcal{L}\{N_p(t)\}(s) = N_p(0)(s^{\beta-1}/(s^\beta + \mu^\beta)) + (\pi^\beta/s(s^\beta + \mu^\beta))$.

Consequently, we have $N_p(t) = (\pi^\beta/\mu^\beta) - ((\pi^\beta/\mu^\beta) - N_p(0))E_\beta(-\mu^\beta t^\beta)$.

It follows that as $t \rightarrow \infty$, $0 \leq N_p \leq (\pi^\beta/\mu^\beta)$, This completes the proof. \square

4. Local Stability

In this section, the local stability analysis of equilibrium points will be covered.

Theorem 13. *The equilibrium points of Model (13) are locally asymptotically stable if the following Matignon condition is satisfied*

$$|\arg(\lambda_j(\mathbb{J}))| > \beta \frac{\pi}{2}, \quad j = 1, 2, \dots, 5, \quad (20)$$

where $\lambda(\mathbb{J})$ stands for the class of all eigenvalues (λ) of the Jacobian matrix (\mathbb{J}) of Model (13).

4.1. Local Stability Analysis of Disease-Free Equilibrium Point. Model's (13) equilibrium points are derived by setting Model's (13) right side to zero. The disease-free equilibrium point is given by $T_p^\circ = (S_\circ, E_p^\circ, A_p^\circ, I_p^\circ, C_\circ) = ((\pi^\beta/\mu^\beta), 0, 0, 0, 0)$.

The threshold value of Model (13) which is known as a basic reproduction number (\mathcal{R}_{p°) can be computed using the next-generation matrix (\mathbb{G}) indicated in Van den Driessche and Watmough [46]. The transmission matrix (F_p) and transition matrix (V_p) of Model (13) are obtained respectively as follows

$$\mathbf{F}_p = \begin{pmatrix} \lambda_p^\beta S \\ 0 \\ 0 \\ 0 \end{pmatrix}, \quad (21)$$

$$\mathbf{V}_p = \begin{pmatrix} \dot{a} E_p \\ -(1-q)\eta^\beta E_p + \dot{d} A_p \\ -q\eta^\beta E_p + \dot{e} I_p \\ -\alpha_3^\beta I_p - w_3^\beta A_p + \mu^\beta C \end{pmatrix}.$$

Then, we compute the derivative of matrices F_p and V_p with respect to infected classes at T_p° , and we get Jacobian of F_p and V_p , respectively so that

$$\mathbf{F}_p = \begin{pmatrix} 0 & \mathcal{B}_p q_p r_3^\beta & \mathcal{B}_p q_p r_4^\beta & 0 \\ 0 & 0 & 0 & 0 \\ 0 & 0 & 0 & 0 \\ 0 & 0 & 0 & 0 \end{pmatrix}, \tag{22}$$

$$\mathbf{V}_p = \begin{pmatrix} \dot{a} & 0 & 0 & 0 \\ -(1-q)\eta^\beta & \dot{d} & 0 & 0 \\ 0 & 0 & \dot{e} & 0 \\ 0 & -w_3^\beta & -\alpha_3^\beta & \mu^\beta \end{pmatrix}.$$

The aforementioned matrices are utilized to determine \mathcal{R}_{p° for Model (13) using the spectral radius (ρ). That is, $\mathcal{R}_{p^\circ} = \rho(\mathbb{G}) = \rho(\mathbf{F}_p \mathbf{V}_p^{-1})$, and is given by

$$\mathcal{R}_{p^\circ} = \frac{\mathcal{B}_p q_p \eta^\beta ((1-q)r_3^\beta \dot{e} + q r_4^\beta \dot{d})}{\dot{a} \dot{e}}. \tag{23}$$

Theorem 14. T_p° is locally asymptotically stable if $\mathcal{R}_{p^\circ} < 1$ and unstable if $\mathcal{R}_{p^\circ} > 1$.

Proof. The linearization matrix of Model (13) around T_p° , is:

$$\mathbb{J}(\mathbb{N}_p(t))|_{T_p^\circ} = \begin{bmatrix} -\mu^\beta & 0 & -\mathcal{B}_p q_p r_3^\beta & -\mathcal{B}_p q_p r_4^\beta & 0 \\ 0 & -\dot{a} & \mathcal{B}_p q_p r_3^\beta & \mathcal{B}_p q_p r_4^\beta & 0 \\ 0 & (1-q)\eta^\beta & -\dot{d} & 0 & 0 \\ 0 & q\eta^\beta & 0 & -\dot{e} & 0 \\ 0 & 0 & w_3^\beta & \alpha_3^\beta & -\mu^\beta \end{bmatrix}, \tag{24}$$

here, $\mathbb{N}_p(t) = (S(t), E_p(t), A_p(t), I_p(t), C(t))$.

Then the characteristic equation of the linearized Model (24) is

$$(\mu^\beta + \lambda)^2 (\lambda^3 + \delta_1 \lambda^2 + \delta_2 \lambda + \delta_3) = 0, \tag{25}$$

where $\delta_1 = \dot{a} + \dot{d} + \dot{e}$, $\delta_2 = \dot{a}\dot{e} + \dot{e}\dot{d} + \dot{a}\dot{d} - \mathcal{B}_p q_p \eta^\beta ((1-q)r_3^\beta + q r_4^\beta)$, and $\delta_3 = \dot{a}\dot{d}\dot{e}(1 - \mathcal{R}_{p^\circ})$.

It is clear that $\lambda_{1,2} = -\mu^\beta$ are negative. The three remaining eigenvalues are the roots of the characteristic equation

$$\lambda^3 + \delta_1 \lambda^2 + \delta_2 \lambda + \delta_3 = 0. \tag{26}$$

The necessary and sufficient conditions on three-order Routh-Hurwitz determinants such that the zeros of (26) have negative real parts or (20) to be satisfied are $\delta_1, \delta_3 > 0$ and $\delta_1 \delta_2 - \delta_3 > 0$.

It is easy to show that

$$\delta_1 = \dot{a} + \dot{d} + \dot{e} > 0, \tag{27}$$

$$\delta_3 = \dot{a}\dot{d}\dot{e}(1 - \mathcal{R}_{p^\circ}) > 0 \text{ if } \mathcal{R}_{p^\circ} < 1, \tag{28}$$

and

$$\delta_1 \delta_2 - \delta_3 = \dot{e}\dot{d}(\dot{a} + \dot{d} + \dot{e}) \left(1 + \frac{\mathcal{B}_p q_p \eta^\beta}{\dot{e}^2 \dot{d}^2} \left((1-q)r_3^\beta \dot{e}^2 + q r_4^\beta \dot{d}^2 \right) \right) + \dot{a} \left(\dot{d}^2 + (\dot{a} + \dot{d})(\dot{a} + \dot{e}) \right) (1 - \mathcal{R}_{p^\circ}) > 0 \text{ if } \mathcal{R}_{p^\circ} < 1. \tag{29}$$

All stability conditions have been met, then, T_p° is locally asymptotically stable if $\mathcal{R}_{p^\circ} < 1$ and unstable if $\mathcal{R}_{p^\circ} > 1$. \square

4.2. Local Stability Analysis of Endemic Equilibrium Point.

The endemic equilibrium point of Model (13) denoted by $T_p^* = (S^*, E_p^*, A_p^*, I_p^*, C^*)$, where $S^* = (\pi^\beta/\mu^\beta)(1/\mathcal{R}_{p_0})$, $E_p^* = (\pi^\beta/\dot{a})((\mathcal{R}_{p_0} - 1)/\mathcal{R}_{p_0})$, $A_p^* = (1 - q)(\eta^\beta \pi^\beta / \dot{a} \dot{d})((\mathcal{R}_{p_0} - 1)/\mathcal{R}_{p_0})$, $I_p^* = q(\eta^\beta \pi^\beta / \dot{a} \dot{e})((\mathcal{R}_{p_0} - 1)/\mathcal{R}_{p_0})$, $C^* = (\eta^\beta \pi^\beta / \mu^\beta \dot{a} \dot{d} \dot{e})((1 - q)\dot{e}w_3^\beta + q\dot{d}\alpha_3^\beta)((\mathcal{R}_{p_0} - 1)/\mathcal{R}_{p_0})$.

Theorem 15. T_p^* is locally asymptotically stable if $\mathcal{R}_{p_0} > 1$ and unstable if $\mathcal{R}_{p_0} < 1$.

Proof. The linearization matrix of Model (13) around T_p^* is

$$\mathbb{J}(\mathbb{N}_p(t))|_{T_p^*} = \begin{bmatrix} \mathfrak{F}_1^* & \mathfrak{F}_2^* & \mathfrak{F}_3^* & \mathfrak{F}_4^* & \mathfrak{F}_5^* \\ \mathfrak{F}_5^* & -\mathfrak{F}_2^* - \dot{a} & -\mathfrak{F}_3^* & -\mathfrak{F}_4^* & -\mathfrak{F}_5^* \\ 0 & (1 - q)\eta^\beta & -\dot{d} & 0 & 0 \\ 0 & q\eta^\beta & 0 & -\dot{e} & 0 \\ 0 & 0 & w_3^\beta & \alpha_3^\beta & -\mu^\beta \end{bmatrix}, \quad (30)$$

here $\mathfrak{F}_1^* = \mu^\beta((-\mathcal{R}_{p_0}^2 + \mathcal{R}_{p_0} - 1)/\mathcal{R}_{p_0})$, $\mathfrak{F}_2^* = \mu^\beta((\mathcal{R}_{p_0} - 1)/\mathcal{R}_{p_0})$, $\mathfrak{F}_3^* = -(\mathcal{B}_p q_p r_3^\beta - \mu^\beta(\mathcal{R}_{p_0} - 1))(1/\mathcal{R}_{p_0})$, $\mathfrak{F}_4^* = -(\mathcal{B}_p q_p r_4^\beta - \mu^\beta(\mathcal{R}_{p_0} - 1))(1/\mathcal{R}_{p_0})$, and $\mathfrak{F}_5^* = \mu^\beta((\mathcal{R}_{p_0} - 1)^2/\mathcal{R}_{p_0})$.

Matrix (30) eigenvalues yield the following fifth-degree polynomial equation

$$(\lambda + \mu^\beta)(\lambda^4 + \mathcal{T}_3\lambda^3 + \mathcal{T}_2\lambda^2 + \mathcal{T}_1\lambda + \mathcal{T}_0) = 0 \quad (31)$$

where $\mathcal{T}_3 = \dot{a} + \dot{d} + \dot{e} + \mu^\beta \mathcal{R}_{p_0}$, $\mathcal{T}_2 = \dot{a}\dot{d} + \dot{a}\dot{e} + \dot{d}\dot{e} + (\dot{a} + \dot{d} + \dot{e})\mu^\beta \mathcal{R}_{p_0} - (\mathcal{B}_p q_p \eta^\beta / \mathcal{R}_{p_0})((1 - q)r_3^\beta + qr_4^\beta)$, $\mathcal{T}_1 = (\dot{d}\dot{e} + \dot{a}(\dot{e} + \dot{d})\mathcal{R}_{p_0})\mu^\beta + 2\dot{d}\dot{e}\mu^\beta((\mathcal{R}_{p_0} - 1)/\mathcal{R}_{p_0}) - (\mathcal{B}_p q_p \eta^\beta \mu^\beta / \mathcal{R}_{p_0})((1 - q)r_3^\beta + qr_4^\beta)$, and $\mathcal{T}_0 = \dot{a}\dot{d}\dot{e}((\mathcal{R}_{p_0} - 1)/\mathcal{R}_{p_0})$.

The following eigenvalue is easily obtained $-\mu^\beta$. The remaining eigenvalues are the roots of the characteristic equation

$$\lambda^4 + \mathcal{T}_3\lambda^3 + \mathcal{T}_2\lambda^2 + \mathcal{T}_1\lambda + \mathcal{T}_0 = 0. \quad (32)$$

The necessary and sufficient conditions on fourth-order Routh-Hurwitz determinants for the zeros of (32) to have negative real parts or (20) to be fulfilled are $\mathcal{T}_0, \mathcal{T}_1, \mathcal{T}_3 > 0$ and $\mathcal{T}_1\mathcal{T}_2\mathcal{T}_3 - \mathcal{T}_1^2 - \mathcal{T}_0\mathcal{T}_3^2 > 0$.

It is simple to establish that $\mathcal{T}_3 > 0$, and $\mathcal{T}_1, \mathcal{T}_0 > 0$ if $\mathcal{R}_{p_0} > 1$.

Finally, we show that $\mathcal{T}_1\mathcal{T}_2\mathcal{T}_3 - \mathcal{T}_1^2 - \mathcal{T}_0\mathcal{T}_3^2 > 0$.

$$\begin{aligned} \mathcal{T}_1\mathcal{T}_2\mathcal{T}_3 - \mathcal{T}_1^2 - \mathcal{T}_0\mathcal{T}_3^2 &= \frac{1}{\mathcal{R}_{p_0}} \left[2\dot{d}\dot{e}\mu^\beta(\dot{a} + \dot{d} + \dot{e}) \left(\mu^{\beta^2} \mathcal{R}_{p_0}^3 - \dot{a}\mathcal{R}_{p_0}^2 - \mathbf{H} \right) \frac{(\mathcal{R}_{p_0} - 1)}{\mathcal{R}_{p_0}} \right. \\ &\quad + \mu^{\beta^2} \mathcal{R}_{p_0}^2 \left[\dot{a}\mu^\beta(\dot{a} + \dot{d} + \dot{e}) \left((\dot{d} + \dot{e})\mathcal{R}_{p_0}^2 - \mathbf{H} \right) - \dot{a}\dot{d}\dot{e}(\mathcal{R}_{p_0} - 1) \right] \\ &\quad + \dot{a}\dot{d}\dot{e}\mu^\beta(\dot{d} + \dot{e})\mathcal{R}_{p_0} \left[(\dot{a} + \dot{d} + \dot{e})\mathcal{R}_{p_0} - 2\mu^\beta(\mathcal{R}_{p_0} - 1) \right] \\ &\quad + \dot{a}(\dot{d} + \dot{e})(\dot{a} + \dot{d} + \dot{e})\mu^\beta \mathcal{R}_{p_0} \left(\dot{a}(\dot{d} + \dot{e})\mathcal{R}_{p_0} - \mathbf{H} \right) \\ &\quad + (\dot{d} + \dot{e})\mu^{\beta^2} \mathcal{R}_{p_0} \left[\dot{d}\dot{e}\mathcal{R}_{p_0}^2 - \dot{a}\mathbf{H}(\mathcal{R}_{p_0} - 1) \right] \\ &\quad + \frac{\dot{d}\dot{e}\mu^{\beta^2}}{\mathcal{R}_{p_0}} \left[\dot{a}\mu^\beta \mathcal{R}_{p_0}^4 + 4\mathbf{H}\mathcal{R}_{p_0} + \mathbf{H}(\mathcal{R}_{p_0} - 1) \right] \\ &\quad + \dot{d}\dot{e}(\dot{a} + \dot{d} + \dot{e})\mu^\beta \left[(\dot{a}\dot{d} + \dot{a}\dot{e} + \dot{d}\dot{e})\mathcal{R}_{p_0} - \mathbf{H} \right] \\ &\quad + (\dot{a} + \dot{d} + \dot{e})^2 \mu^{\beta^2} \mathcal{R}_{p_0} \left[(\dot{a}\dot{d} + \dot{a}\dot{e})\mathcal{R}_{p_0}^2 - \mathbf{H} \right] \\ &\quad + 2\dot{d}^2 \dot{e}^2 \mu^\beta \left[(\eta^\beta + w_3^\beta + \alpha_3^\beta)\mathcal{R}_{p_0} + 2\mu^\beta \right] \frac{(\mathcal{R}_{p_0} - 1)}{\mathcal{R}_{p_0}} \\ &\quad + 2\dot{a}\dot{d}\dot{e}\mu^\beta(\dot{a} + \dot{d} + \dot{e})(\dot{d} + \dot{e})(\mathcal{R}_{p_0} - 1) + \dot{d}\dot{e}(\dot{a} + \dot{d} + \dot{e})^2 \mu^{\beta^2} \mathcal{R}_{p_0} \\ &\quad \left. + \mathbf{H} \left(2\dot{d}\dot{e} + \mu^{\beta^2} \mathbf{H} \right) \frac{(\mathcal{R}_{p_0} - 1)}{\mathcal{R}_{p_0}} + (\dot{a} + \dot{d} + \dot{e})\mu^\beta \frac{\mathbf{H}^2}{\mathcal{R}_{p_0}} \right] > 0, \text{ if } \mathcal{R}_{p_0} > 1, \end{aligned} \quad (33)$$

where $\mathbf{H} = \mathcal{B}_p q_p \eta^\beta ((1-q)r_3^\beta + qr_4^\beta)$. T_p^* has just been demonstrated to be locally asymptotically stable if $\mathcal{R}_{p_0} > 1$ and unstable if $\mathcal{R}_{p_0} < 1$. \square

5. Global Stability

In this section, we examine the global stability for model (13) by building appropriate Lyapunov functions. In order

to show global stability, we take the function $0 \leq Y(z) = z - 1 - \ln(z), \forall z > 0$ into consideration.

Lemma 16 (see [47]). *Assume $g(t) \in \mathbb{R}_{\geq 0}$ be a continuous function. Then, for any time $t \geq 0$*

$$g^* \text{ } {}_0^c D_t^\beta Y(g(t)) \leq \left(1 - \frac{g^*}{g(t)}\right) {}_0^c D_t^\beta g(t), g^* \in \mathbb{R}_{\geq 0}, \forall \beta \in (0, 1). \tag{34}$$

Theorem 17. T_p° is globally asymptotically stable whenever $\mathcal{R}_{p_0} < 1$.

Proof. Suppose the following Lyapunov function:

$$\begin{aligned} V_p^\circ(t) = V_p^\circ(\mathbb{N}_p(t)) = & S_0 Y\left(\frac{S(t)}{S_0}\right) + E_p(t) + \left(\frac{\mathcal{B}_p q_p r_3^\beta \mu^\beta}{\dot{a}d} + 1\right) A_p(t) \\ & + \left(\frac{\mathcal{B}_p q_p r_4^\beta \mu^\beta}{\dot{a}e} + 1\right) I_p(t) + C(t). \end{aligned} \tag{35}$$

Clearly, $V_p^\circ(t) > 0, \forall S(t), E_p(t), A_p(t), I_p(t), C(t) > 0$ and $V_p^\circ(t)|_{T_p^\circ} = 0$.

Calculate ${}_0^c D_t^\beta V_p^\circ(t)$ along the solution of model (13) as

$$\begin{aligned} {}_0^c D_t^\beta V_p^\circ(t) = & S_0 {}_0^c D_t^\beta Y\left(\frac{S(t)}{S_0}\right) + {}_0^c D_t^\beta E_p(t) + \left(\frac{\mathcal{B}_p q_p r_3^\beta \mu^\beta}{\dot{a}d} + 1\right) {}_0^c D_t^\beta A_p(t) \\ & + \left(\frac{\mathcal{B}_p q_p r_4^\beta \mu^\beta}{\dot{a}e} + 1\right) {}_0^c D_t^\beta I_p(t) + {}_0^c D_t^\beta C(t) \\ \leq & \left(1 - \frac{S_0}{S(t)}\right) (\pi^\beta - (\lambda_p^\beta + \mu^\beta) S(t)) \\ & + \lambda_p^\beta S(t) - (\eta^\beta + \mu^\beta) E_p(t) \\ & + \left(\frac{\mathcal{B}_p q_p r_3^\beta \mu^\beta}{\dot{a}d} + 1\right) ((1-q)\eta^\beta E_p(t) - (w_3^\beta + \mu^\beta) A_p(t)) \\ & + \left(\frac{\mathcal{B}_p q_p r_4^\beta \mu^\beta}{\dot{a}e} + 1\right) (q\eta^\beta E_p(t) - (\alpha_3^\beta + \mu^\beta) I_p(t)) \\ & + \alpha_3^\beta I_p(t) + w_3^\beta A_p(t) - \mu^\beta C(t) \\ = & -\mu^\beta \frac{(S(t) - S_0)^2}{S(t)} + \lambda_p^\beta S_0 - \frac{\mathcal{B}_p q_p \mu^\beta}{\dot{a}} (r_3^\beta A_p(t) + r_4^\beta I_p(t)) \end{aligned}$$

$$\begin{aligned}
& + \mu^\beta \left(\mathcal{R}_{p_0} q_p \eta^\beta \left(\frac{(1-q)r_3^\beta \dot{e} + q r_4^\beta \dot{d}}{\dot{a} \dot{e}} \right) - 1 \right) E_p(t) \\
& - \mu^\beta (A_p(t) + I_p(t) + C(t)) \\
= & \mu^\beta \left(-\frac{(S(t) - S_0)^2}{S(t)} + (\mathcal{R}_{p_0} - 1) E_p(t) - (A_p(t) + I_p(t) + C(t)) \right) \\
& - \mu^\beta \lambda_p^\beta \left(\frac{N_p(t)}{\dot{a}} - \frac{S_0}{\mu^\beta} \right).
\end{aligned} \tag{36}$$

Therefore, $\mathcal{R}_{p_0} < 1$ guarantees for all $S(t)$, $E_p(t)$, $A_p(t)$, $I_p(t)$, $C(t) > 0$ that ${}^c_0 D_t^\beta V_p^\circ(t) \leq 0$, $\forall t \geq 0$.

Moreover, it is easy to confirm that ${}^c_0 D_t^\beta V_p^\circ(t)|_{T_p^c} = 0$. Hence, T_p^c is the largest compact invariant subset of $\Pi_p^\circ = \{N_p(t) \in \mathbb{R}_{\geq 0}^5 : {}^c_0 D_t^\beta V_p^\circ(t) = 0\}$. We conclude that T_p^c is globally asymptotically stable provided $\mathcal{R}_{p_0} < 1$ as a result of LaSalle's invariance principle [48]. \square

Theorem 18. T_p^* is globally asymptotically stable when $\mathcal{R}_{p_0} > 1$.

Proof. Let us construct the following Lyapunov function:

$$\begin{aligned}
V_p^*(t) = V_p^\circ(N_p(t)) &= \frac{\dot{a}}{2(\dot{a} + \mu^\beta) S^*} (S(t) - S^* + E_p(t) - E_p^*)^2 + S^* \Upsilon \left(\frac{S(t)}{S^*} \right) \\
& + E_p^* \Upsilon \left(\frac{E_p(t)}{E_p^*} \right) + A_p^* \Upsilon \left(\frac{A_p(t)}{A_p^*} \right) \\
& + I_p^* \Upsilon \left(\frac{I_p(t)}{I_p^*} \right) + \Upsilon \left(\frac{C(t)}{C^*} \right).
\end{aligned} \tag{37}$$

Obviously, $V_p^*(t) > 0$, $\forall S(t), E_p(t), A_p(t), I_p(t), C(t) > 0$ and $V_p^*(t)|_{T_p^*} = 0$. Evaluate ${}^c_0 D_t^\beta V_p^*(t)$ along the trajectories of model (13), yields

$$\begin{aligned}
{}^c_0 D_t^\beta V_p^*(t) &\leq \frac{\dot{a}}{(\dot{a} + \mu^\beta) S^*} (S(t) - S^* + E_p(t) - E_p^*) {}^c_0 D_t^\beta (S(t) + E_p(t)) \\
& + \left(1 - \frac{S^*}{S(t)} \right) {}^c_0 D_t^\beta S(t) + \left(1 - \frac{E_p^*}{E_p(t)} \right) {}^c_0 D_t^\beta E_p(t) \\
& + \left(1 - \frac{A_p^*}{A_p(t)} \right) {}^c_0 D_t^\beta A_p(t) + \left(1 - \frac{I_p^*}{I_p(t)} \right) {}^c_0 D_t^\beta I_p(t) \\
& + \left(1 - \frac{C^*}{C(t)} \right) {}^c_0 D_t^\beta C(t).
\end{aligned} \tag{38}$$

At T_p^* , we possess $\pi^\beta = \mu^\beta S^* + \dot{a} E_p^*$, $\dot{a} E_p^* = \lambda_p^{\beta} S^*$, $\dot{d} A_p^* = (1 - q)\eta^\beta E_p^*$, and $\dot{e} I_p^* = q\eta^\beta E_p^*$, where $\lambda_p^{\beta} = (\mathcal{B}_p q_p (r_3^\beta A_p^* + r_4^\beta I_p^*) / (S^* + E_p^* + A_p^* + I_p^* + C^*))$. Then

$$\begin{aligned}
 {}_0^c D_t^\beta V_p^*(t) &\leq -\frac{\dot{a}\mu^\beta}{(\dot{a} + \mu)S^*}(S(t) - S^*)^2 - \mu^\beta \frac{(S(t) - S^*)^2}{S(t)} - \frac{\dot{a}^2}{(\dot{a} + \mu)S^*}(E_p(t) - E_p^*)^2 \\
 &+ \dot{a}E_p(t) \left(3 - \frac{S(t)}{S^*} - \frac{S^* E_p^*}{S(t)E_p(t)} - \frac{E_p(t)}{E_p^*} \right) - \dot{a}E_p(t) + \dot{a}E_p^* \frac{S(t)}{S^*} + \lambda_p^\beta S^* \\
 &- \lambda_p^\beta S \frac{E_p^*}{E_p(t)} + \dot{a} \frac{(E_p(t) - E_p^*)^2}{E_p^*} + \dot{d}A_p^* \left(3 - \frac{A_p^* E_p(t)}{A_p(t)E_p^*} - \frac{A_p(t)}{A_p^*} - \frac{E_p^*}{E_p(t)} \right) \\
 &+ \dot{d}A_p^* \left(\frac{E_p^*}{E_p(t)} - 2 \right) + \dot{e}I_p^* \left(3 - \frac{I_p^* E_p(t)}{I_p(t)E_p^*} - \frac{I_p(t)}{I_p^*} - \frac{E_p^*}{E_p(t)} \right) \\
 &+ \dot{e}I_p^* \left(\frac{E_p^*}{E_p(t)} - 2 \right) + w_3^\beta A_p(t) \left(3 - \frac{A_p^* C(t)}{A_p(t)C^*} - \frac{A_p(t)}{A_p^*} - \frac{C^*}{C(t)} \right) \\
 &+ \alpha_3^\beta I_p(t) \left(3 - \frac{I_p^* C(t)}{I_p(t)C^*} - \frac{I_p(t)}{I_p^*} - \frac{C^*}{C(t)} \right) \\
 &+ w_3^\beta \frac{(A_p(t) - A_p^*)^2}{A_p^*} + \alpha_3^\beta \frac{(I_p(t) - I_p^*)^2}{I_p^*} \\
 &< -\frac{\dot{a}\mu^\beta}{(\dot{a} + \mu)S^*}(S(t) - S^*)^2 - \mu^\beta \frac{(S(t) - S^*)^2}{S(t)} - \frac{\dot{a}^2}{(\dot{a} + \mu)S^*}(E_p(t) - E_p^*)^2 \\
 &+ \dot{a}E_p(t) \left(3 - \frac{S(t)}{S^*} - \frac{S^* E_p^*}{S(t)E_p(t)} - \frac{E_p(t)}{E_p^*} \right) + \lambda_p^\beta S(t) \left(1 - \frac{S^* E_p(t)}{S(t)E_p^*} \right) \\
 &+ \lambda_p^\beta S^* \left(1 - \frac{S(t)E_p^*}{S^* E_p(t)} \right) + \dot{d}A_p^* \left(3 - \frac{A_p^* E_p(t)}{A_p(t)E_p^*} - \frac{A_p(t)}{A_p^*} - \frac{E_p^*}{E_p(t)} \right) \\
 &+ \dot{e}I_p^* \left(3 - \frac{I_p^* E_p(t)}{I_p(t)E_p^*} - \frac{I_p(t)}{I_p^*} - \frac{E_p^*}{E_p(t)} \right) + \dot{a}E_p^* \left(\frac{E_p^*}{E_p(t)} - 1 \right) \\
 &+ \dot{a} \frac{(E_p(t) - E_p^*)^2}{E_p^*} + w_3^\beta A_p(t) \left(3 - \frac{A_p^* C(t)}{A_p(t)C^*} - \frac{A_p(t)}{A_p^*} - \frac{C^*}{C(t)} \right) \\
 &+ \alpha_3^\beta I_p(t) \left(3 - \frac{I_p^* C(t)}{I_p(t)C^*} - \frac{I_p(t)}{I_p^*} - \frac{C^*}{C(t)} \right) \\
 &< -\mu^\beta \left(\frac{\dot{a}S(t)}{(\dot{a} + \mu)} + S^* \right) \frac{(S(t) - S^*)^2}{S(t)S^*} - \frac{\dot{a}^2}{(\dot{a} + \mu)S^*}(E_p(t) - E_p^*)^2 \\
 &+ \dot{a}E_p(t) \left(3 - \frac{S(t)}{S^*} - \frac{S^* E_p^*}{S(t)E_p(t)} - \frac{E_p(t)}{E_p^*} \right) \\
 &+ \dot{a}E_p^* \left(2 - \frac{S^* E_p(t)}{S(t)E_p^*} - \frac{S(t)E_p^*}{S^* E_p(t)} \right) + \dot{d}A_p^* \left(3 - \frac{A_p^* E_p(t)}{A_p(t)E_p^*} - \frac{A_p(t)}{A_p^*} - \frac{E_p^*}{E_p(t)} \right) \\
 &+ \dot{e}I_p^* \left(3 - \frac{I_p^* E_p(t)}{I_p(t)E_p^*} - \frac{I_p(t)}{I_p^*} - \frac{E_p^*}{E_p(t)} \right) + w_3^\beta A_p(t) \left(3 - \frac{A_p^* C(t)}{A_p(t)C^*} - \frac{A_p(t)}{A_p^*} - \frac{C^*}{C(t)} \right) \\
 &+ \alpha_3^\beta I_p(t) \left(3 - \frac{I_p^* C(t)}{I_p(t)C^*} - \frac{I_p(t)}{I_p^*} - \frac{C^*}{C(t)} \right)
 \end{aligned} \tag{39}$$

which according to the arithmetic mean-geometric mean inequality, is less than or equal to zero. Thus, $\mathcal{R}_{p_0} > 1$ ensures for all $S(t), E_p(t), A_p(t), I_p(t), C(t) > 0$ that

$${}^c_0 D_t^\beta V_p^*(t) \leq 0, \quad \forall t \geq 0. \quad (40)$$

Further, it is clear that ${}^c_0 D_t^\beta V_p^*(t)|_{T_p^*} = 0$. Therefore, T_p^* is the largest compact invariant subset of $\Pi_p^* = \{\mathbb{N}_p(t) \in \mathbb{R}_{\geq 0}^5: {}^c_0 D_t^\beta V_p^*(t) = 0\}$. According to LaSalle's invariance principle [48], T_p^* is globally asymptotically stable so long as $\mathcal{R}_{p_0} > 1$. \square

6. Construction of Finite Difference Scheme

To acquire numerical solutions for HPV-CC fractional-order model (13), we create the finite difference scheme in this section. To estimate the fractional derivative, one can utilize Grünwald-Letnikov approach. The suggested finite difference scheme maintains the positivity and stability of the equilibrium points of the solution corresponding to the continuous epidemiological models of fractional order.

Let $t \in [0, \mathbb{T}]$, a finite interval. The usual notation $t_k = k\delta_t, k = 0, 1, \dots, N$ and $u(t_k) \equiv u_k$ are used, where $\delta_t = (\mathbb{T}/N)$ and u_k denotes the numerical solution of the analytical solution of $u(t)$ at the grid points t_k .

Grünwald-Letnikov discretization approach based on Caputo derivative is defined as

$${}^c_0 D_t^\beta u_k = \frac{1}{\delta_t^\beta} \left(u_{k+1} - \sum_{j=1}^{k+1} d_j^{(\beta)} u_{k+1-j} - \vartheta_{k+1}^\beta u_0 \right), \quad \forall \beta \in (0, 1), \quad (41)$$

where $d_j^{(\beta)} = (-1)^{j-1} \binom{\beta}{j}, d_1^{(\beta)} = \beta,$ and $\vartheta_j^\beta = (j^{-\beta}/\Gamma(1-\beta)), \vartheta_1^\beta = (1/\Gamma(1-\beta)), j = 1, 2, \dots, k+1.$

Lemma 19 (see [49]). *Suppose that $\beta \in (0, 1)$, therefore the coefficients $d_j^{(\beta)}$ and ϑ_j^β fulfil for $j \geq 1$ the properties*

$$0 < d_{j+1}^{(\beta)} < d_j^{(\beta)} < \dots < d_1^{(\beta)} = \beta < 1,$$

$$0 < \vartheta_{j+1}^\beta < \vartheta_j^\beta < \dots < \vartheta_1^\beta = \frac{1}{\Gamma(1-\beta)}, \quad (42)$$

$$\sum_{j=1}^{\infty} d_j^{(\beta)} = 1.$$

The finite difference scheme of Model (13) using Grünwald-Letnikov discretization approach (41) is as follows

$$\left\{ \begin{array}{l} \frac{1}{\delta_t^\beta} \left(S_{k+1} - \sum_{j=1}^{k+1} d_j^{(\beta)} S_{k+1-j} - \vartheta_{k+1}^\beta S_0 \right) = \pi^\beta - (\lambda_{p_k}^\beta + \mu^\beta) S_{k+1}, \\ \frac{1}{\delta_t^\beta} \left(E_{p_{k+1}} - \sum_{j=1}^{k+1} d_j^{(\beta)} E_{p_{k+1-j}} - \vartheta_{k+1}^\beta E_{p_0} \right) = \lambda_{p_k}^\beta S_{k+1} - \dot{a} E_{p_{k+1}}, \\ \frac{1}{\delta_t^\beta} \left(A_{p_{k+1}} - \sum_{j=1}^{k+1} d_j^{(\beta)} A_{p_{k+1-j}} - \vartheta_{k+1}^\beta A_{p_0} \right) = (1-q)\eta^\beta E_{p_{k+1}} - \dot{d} A_{p_{k+1}}, \\ \frac{1}{\delta_t^\beta} \left(I_{p_{k+1}} - \sum_{j=1}^{k+1} d_j^{(\beta)} I_{p_{k+1-j}} - \vartheta_{k+1}^\beta I_{p_0} \right) = q\eta^\beta E_{p_{k+1}} - \dot{e} I_{p_{k+1}}, \\ \frac{1}{\delta_t^\beta} \left(C_{k+1} - \sum_{j=1}^{k+1} d_j^{(\beta)} C_{k+1-j} - \vartheta_{k+1}^\beta C_0 \right) = \alpha_3^\beta I_{p_{k+1}} + w_3^\beta A_{p_{k+1}} - \mu^\beta C_{k+1}, \end{array} \right. \quad (43)$$

here $\lambda_{p_k}^\beta = (\mathcal{B}_p q_p (r_3^\beta A_{p_k} + r_4^\beta I_{p_k})/N_{p_k}), N_{p_k} = S_k + E_{p_k} + A_{p_k} + I_{p_k} + C_k.$

Because each of these equations is linear in $S_{k+1}, E_{p_{k+1}}, A_{p_{k+1}}, I_{p_{k+1}}$, and C_{k+1} , hence through some calculations the following explicit expressions can be obtained

$$\left\{ \begin{aligned} S_{k+1} &= \frac{1}{1 + \delta_t^\beta (\lambda_{p_k}^\beta + \mu^\beta)} \left[\sum_{j=1}^{k+1} d_j^{(\beta)} S_{k+1-j} + \vartheta_{k+1}^\beta S_0 + \delta_t^\beta \pi^\beta \right], \\ E_{p_{k+1}} &= \frac{1}{1 + \delta_t^\beta \dot{a}} \left[\sum_{j=1}^{k+1} d_j^{(\beta)} E_{p_{k+1}-j} + \vartheta_{k+1}^\beta E_{p_0} + \delta_t^\beta \lambda_{p_k}^\beta S_{k+1} \right], \\ A_{p_{k+1}} &= \frac{1}{1 + \delta_t^\beta \dot{d}} \left[\sum_{j=1}^{k+1} d_j^{(\beta)} A_{p_{k+1}-j} + \vartheta_{k+1}^\beta A_{p_0} + \delta_t^\beta (1 - q) \eta^\beta E_{p_{k+1}} \right], \\ I_{p_{k+1}} &= \frac{1}{1 + \delta_t^\beta \dot{e}} \left[\sum_{j=1}^{k+1} d_j^{(\beta)} I_{p_{k+1}-j} + \vartheta_{k+1}^\beta I_{p_0} + \delta_t^\beta q \eta^\beta E_{p_{k+1}} \right], \\ C_{k+1} &= \frac{1}{1 + \delta_t^\beta \mu^\beta} \left[\sum_{j=1}^{k+1} d_j^{(\beta)} C_{k+1-j} + \vartheta_{k+1}^\beta C_0 + \delta_t^\beta \alpha_3^\beta I_{p_{k+1}} + \delta_t^\beta w_3^\beta A_{p_{k+1}} \right]. \end{aligned} \right. \tag{44}$$

6.1. Non-Negativity and Boundedness of Finite Difference Scheme. This subsection examines a few characteristics of proposed Scheme (44). Keeping in mind that system (13) have unique non-negative solutions and also all the parameters are positive.

Theorem 20 (Non-negativity). *Assume that in (44) $S_0 \geq 0, E_{p_0} \geq 0, A_{p_0} \geq 0, I_{p_0} \geq 0$, and $C_0 \geq 0$, then $S_k > 0, E_{p_k} > 0, A_{p_k} > 0, I_{p_k} > 0$, and $C_k > 0$ is satisfied for all $k = 1, 2, \dots, N$.*

Proof. The induction will be used to prove this theorem. For $k = 0$ in Scheme (44), we get

$$\left\{ \begin{aligned} S_1 &= \frac{1}{1 + \delta_t^\beta (\lambda_{p_0}^\beta + \mu^\beta)} \left[d_1^{(\beta)} S_0 + \vartheta_1^\beta S_0 + \delta_t^\beta \pi^\beta \right] > 0, \\ E_{p_1} &= \frac{1}{1 + \delta_t^\beta \dot{a}} \left[d_1^{(\beta)} E_{p_0} + \vartheta_1^\beta E_{p_0} + \delta_t^\beta \lambda_{p_0}^\beta S_1 \right] > 0, \\ A_{p_1} &= \frac{1}{1 + \delta_t^\beta \dot{d}} \left[d_1^{(\beta)} A_{p_0} + \vartheta_1^\beta A_{p_0} + \delta_t^\beta (1 - q) \eta^\beta E_{p_1} \right] > 0, \\ I_{p_1} &= \frac{1}{1 + \delta_t^\beta \dot{e}} \left[d_1^{(\beta)} I_{p_0} + \vartheta_1^\beta I_{p_0} + \delta_t^\beta q \eta^\beta E_{p_1} \right] > 0, \\ C_1 &= \frac{1}{1 + \delta_t^\beta \mu^\beta} \left[d_1^{(\beta)} C_0 + \vartheta_1^\beta C_0 + \delta_t^\beta \alpha_3^\beta I_{p_1} + \delta_t^\beta w_3^\beta A_{p_1} \right] > 0. \end{aligned} \right. \tag{45}$$

We presume that in system (44), $S_k > 0, E_{p_k} > 0, A_{p_k} > 0, I_{p_k} > 0$, and $C_k > 0 \forall k < k + 1$. So, for $k + 1$

$$\left\{ \begin{array}{l} S_{k+1} = \frac{1}{1 + \delta_t^\beta (\lambda_{p_k}^\beta + \mu^\beta)} \left[\sum_{j=1}^{k+1} d_j^{(\beta)} S_{k+1-j} + \vartheta_{k+1}^\beta S_0 + \delta_t^\beta \pi^\beta \right] > 0, \\ E_{p_{k+1}} = \frac{1}{1 + \delta_t^\beta \dot{a}} \left[\sum_{j=1}^{k+1} d_j^{(\beta)} E_{p_{k+1-j}} + \vartheta_{k+1}^\beta E_{p_0} + \delta_t^\beta \lambda_{p_k}^\beta S_{k+1} \right] > 0, \\ A_{p_{k+1}} = \frac{1}{1 + \delta_t^\beta \dot{a}} \left[\sum_{j=1}^{k+1} d_j^{(\beta)} A_{p_{k+1-j}} + \vartheta_{k+1}^\beta A_{p_0} + \delta_t^\beta (1 - q) \eta^\beta E_{p_{k+1}} \right] > 0, \\ I_{p_{k+1}} = \frac{1}{1 + \delta_t^\beta \dot{e}} \left[\sum_{j=1}^{k+1} d_j^{(\beta)} I_{p_{k+1-j}} + \vartheta_{k+1}^\beta I_{p_0} + \delta_t^\beta q \eta^\beta E_{p_{k+1}} \right] > 0, \\ C_{k+1} = \frac{1}{1 + \delta_t^\beta \mu^\beta} \left[\sum_{j=1}^{k+1} d_j^{(\beta)} C_{k+1-j} + \vartheta_{k+1}^\beta C_0 + \delta_t^\beta \alpha_3^\beta I_{p_{k+1}} + \delta_t^\beta w_3^\beta A_{p_{k+1}} \right] > 0. \end{array} \right. \quad (46)$$

□

Theorem 21 (boundedness). *Assume that in Scheme (44) $S_0 + E_{p_0} + A_{p_0} + I_{p_0} + C_0 = 1$. Then there exists a constant*

$$\mathbb{M}(k + 1, \beta) = \frac{\beta + ((k + 1)/\Gamma(1 - \beta)) + \delta_t^\beta \pi^\beta}{1 + \delta_t^\beta \mu^\beta}, \quad k = 0, 1, 2, \dots, N, \beta \in (0, 1), \quad (47)$$

such that $S_{k+1}, E_{p_{k+1}}, A_{p_{k+1}}, I_{p_{k+1}}, C_{k+1} \leq \mathbb{M}(k + 1, \beta)$.

Proof. When each equation in Scheme (44) is multiplied by its denominator, the result is

$$N_{p_{k+1}} = \frac{\sum_{j=1}^{k+1} d_j^{(\beta)} N_{p_{k+1-j}} + \vartheta_{k+1}^\beta + \delta_t^\beta \pi^\beta}{1 + \delta_t^\beta \mu^\beta}, \quad (48)$$

here $N_{p_{k+1}} = S_{k+1} + E_{p_{k+1}} + A_{p_{k+1}} + I_{p_{k+1}} + C_{k+1}$, and $N_{p_{k+1-j}} = S_{k+1-j} + E_{p_{k+1-j}} + A_{p_{k+1-j}} + I_{p_{k+1-j}} + C_{k+1-j}$.

Applying the induction principle and utilizing Lemma (19), it follows that for $k = 0$

$$\begin{aligned} S_1 + E_{p_1} + A_{p_1} + I_{p_1} + C_1 &= \frac{\dot{a}_1^{(\beta)} + \vartheta_1^\beta + \delta_t^\beta \pi^\beta}{1 + \delta_t^\beta \mu^\beta} \\ &= \frac{\beta + 1/\Gamma(1 - \beta) + \delta_t^\beta \pi^\beta}{1 + \delta_t^\beta \mu^\beta} := \mathbb{M}(1, \beta). \end{aligned} \quad (49)$$

For $k = 1$, we have

$$\begin{aligned}
 S_2 + E_{p_2} + A_{p_2} + I_{p_2} + C_2 &= \frac{d_1^{(\beta)}(S_1 + E_{p_1} + A_{p_1} + I_{p_1} + C_1) + d_2^{(\beta)} + \vartheta_2^\beta + \delta_t^\beta \pi^\beta}{1 + \delta_t^\beta \mu^\beta} \\
 &< \frac{d_1^{(\beta)} \mathbb{M}(1, \beta) + d_2^{(\beta)} + \vartheta_1^\beta + \delta_t^\beta \pi^\beta}{1 + \delta_t^\beta \mu^\beta} \\
 &< \frac{\mathbb{M}(1, \beta)(d_1^{(\beta)} + d_2^{(\beta)}) + (1/\Gamma(1 - \beta)) + \delta_t^\beta \pi^\beta}{1 + \delta_t^\beta \mu^\beta} \\
 &< \frac{\mathbb{M}(1, \beta) \sum_{j=1}^\infty d_j^{(\beta)} + (1/\Gamma(1 - \beta)) + \delta_t^\beta \pi^\beta}{1 + \delta_t^\beta \mu^\beta} \\
 &= \frac{\mathbb{M}(1, \beta) + (1/\Gamma(1 - \beta)) + \delta_t^\beta \pi^\beta}{1 + \delta_t^\beta \mu^\beta} \\
 &< \frac{\beta + (2/\Gamma(1 - \beta)) + \delta_t^\beta \pi^\beta}{1 + \delta_t^\beta \mu^\beta} := \mathbb{M}(2, \beta).
 \end{aligned} \tag{50}$$

For $k = 2$, we have

$$\begin{aligned}
 S_3 + E_{p_3} + A_{p_3} + I_{p_3} + C_3 &= \frac{d_1^{(\beta)} N_{p_2} + d_2^{(\beta)} N_{p_1} + d_3^{(\beta)} + \vartheta_3^\beta + \delta_t^\beta \pi^\beta}{1 + \delta_t^\beta \mu^\beta} \\
 &< \frac{d_1^{(\beta)} \mathbb{M}(2, \beta) + d_2^{(\beta)} \mathbb{M}(1, \beta) + d_3^{(\beta)} + \vartheta_1^\beta + \delta_t^\beta \pi^\beta}{1 + \delta_t^\beta \mu^\beta} \\
 &< \frac{\mathbb{M}(2, \beta)(d_1^{(\beta)} + d_2^{(\beta)} + d_3^{(\beta)}) + (1/\Gamma(1 - \beta)) + \delta_t^\beta \pi^\beta}{1 + \delta_t^\beta \mu^\beta} \\
 &< \frac{\mathbb{M}(2, \beta) \sum_{j=1}^\infty d_j^{(\beta)} + (1/\Gamma(1 - \beta)) + \delta_t^\beta \pi^\beta}{1 + \delta_t^\beta \mu^\beta} \\
 &= \frac{\mathbb{M}(2, \beta) + (1/\Gamma(1 - \beta)) + \delta_t^\beta \pi^\beta}{1 + \delta_t^\beta \mu^\beta} \\
 &< \frac{\beta + (3/\Gamma(1 - \beta)) + \delta_t^\beta \pi^\beta}{1 + \delta_t^\beta \mu^\beta} := \mathbb{M}(3, \beta),
 \end{aligned} \tag{51}$$

here, $N_{p_2} = S_2 + E_{p_2} + A_{p_2} + I_{p_2} + C_2$ and $N_{p_1} = S_1 + E_{p_1} + A_{p_1} + I_{p_1} + C_1$.

Now, we assume that for $k = 3, \dots, N - 1$, is

$$S_{k+1} + E_{p_{k+1}} + A_{p_{k+1}} + I_{p_{k+1}} + C_{k+1} < \frac{\mathbb{M}(k, \beta) + (1/\Gamma(1 - \beta)) + \delta_t^\beta \pi^\beta}{1 + \delta_t^\beta \mu^\beta} := \mathbb{M}(k + 1, \beta). \tag{52}$$

Thus for $k = N$, we get

TABLE 2: Parameter values for the numerical simulations.

Parameter	Value when $\mathcal{R}_{p_0} < 1$	Value when $\mathcal{R}_{p_0} > 1$	Source
π	16360000	16360000	Assumed
μ	0.6	0.6	Assumed
η	0.21	0.21	Assumed
α_3	0.011	0.011	[42]
w_3	0.039	0.039	[42]
r_4	0.0531	0.590	Assumed
r_3	0.0376	0.376	Assumed
q	0.091	0.967	Assumed
\mathcal{B}_p	0.41	5.0	Assumed
q_p	Varied	Varied	Assumed

$$\begin{aligned}
 N_{p_{N+1}} &= \frac{\sum_{j=1}^{N+1} d_j^{(\beta)} N_{p_{N+1-j}} + g_{N+1}^\beta + \delta_t^\beta \pi^\beta}{1 + \delta_t^\beta \mu^\beta} \\
 &\leq \frac{\mathbb{M}(N, \beta) \sum_{j=1}^\infty d_j^{(\beta)} + (1/\Gamma(1 - \beta)) + \delta_t^\beta \pi^\beta}{1 + \delta_t^\beta \mu^\beta} \\
 &< \frac{\beta + (N + 1)/\Gamma(1 - \beta) + \delta_t^\beta \pi^\beta}{1 + \delta_t^\beta \mu^\beta} := \mathbb{M}(N + 1, \beta),
 \end{aligned}
 \tag{53}$$

here, $N_{p_{N+1}} = S_{N+1} + E_{p_{N+1}} + A_{p_{N+1}} + I_{p_{N+1}} + C_{N+1}$ and $N_{p_{N+1-j}} = S_{N+1-j} + E_{p_{N+1-j}} + A_{p_{N+1-j}} + I_{p_{N+1-j}} + C_{N+1-j}$. Thus, $S_{k+1}, E_{p_{k+1}}, A_{p_{k+1}}, I_{p_{k+1}}, C_{k+1} \leq \mathbb{M}(k + 1, \beta)$, for $k = 0, 1, \dots, N$. \square

6.2. *Stability of Finite Difference Scheme.* This subsection investigates the stability of Scheme (44).

Definition 22. Scheme (44) is said to be asymptotically stable, if there exist constants $\mathbb{L}_1, \mathbb{L}_2, \mathbb{L}_3, \mathbb{L}_4$, and \mathbb{L}_5 as $\beta \rightarrow 1^-$, such that $S_{k+1} \leq \mathbb{L}_1, E_{p_{k+1}} \leq \mathbb{L}_2, A_{p_{k+1}} \leq \mathbb{L}_3, I_{p_{k+1}} \leq \mathbb{L}_4$, and $C_{k+1} \leq \mathbb{L}_5$, Leads for any arbitrary initial values $0 < S_0 + E_{p_0} + A_{p_0} + I_{p_0} + C_0 = 1$, and $k = 0, 1, \dots, N$.

Theorem 23. Assume that the supposition of Theorems (20) and (21) are provided. Hence, Scheme (44) is asymptotically stable.

Proof. According to Theorem (21), we deduce that Scheme (44) is asymptotically stable. \square

7. Numerical Simulations

There are no general techniques for solving systems of fractional differential equations analytically, similar to the classical theory of differential equations. The fractional case is much more challenging to treat even approximately [50]. There are various techniques based on a continuous expansion formula for the fractional derivative that, in some circumstances, can be used to approximately solve the original fractional-order model [51].

In this section, we'll simulate the solution to HPV-CC fractional-order Model (13) using suggested Scheme (44). The presented model's parameter values are either extrapolated from earlier model studies or based on assumptions. Table 2 lists the values of these parameters for the two scenarios $\mathcal{R}_{p_0} < 1$ and $\mathcal{R}_{p_0} > 1$.

Proposed Scheme (44) is implemented with a time step size $\delta_t = 0.02$, and figures of the numerical solutions are presented using varied initial conditions that satisfy Theorem 22 and various values of q_p and derivative order $\beta (\in 0, 1]$.

The convergence of all solutions toward the equilibrium point T_p° is depicted in Figures 2–4 across a range of different values for $\beta (\in 0, 1]$ and q_p . This result was attained when $\mathcal{R}_{p_0} < 1$. The infected classes converge to zero over time while the susceptible compartment ($S(t)$) rises initially and then converges to $S_0 = (\pi^\beta / \mu^\beta)$. T_p° is thereby shown to be globally asymptotically stable. When $\mathcal{R}_{p_0} > 1$, all solutions converge toward the equilibrium point T_p^* which is globally asymptotically stable. This result is shown in Figures 5–7 for a variety of $\beta (\in 0, 1]$ and q_p values indicating that upon the introduction of HPV, the susceptible compartment (S) over time (t) gradually reduces and stays constant and can't be treated. While the exposed compartment (E_p), the asymptomatic compartment (A_p), the infected compartment (I_p), and the compartment affected by cervical cancer (C) gradually increase with time (t).

Consider HPV-CC fractional-order Model (13) with initial condition $(S(0), E_p(0), A_p(0), I_p(0), C(0)) = (0.5425, 0.2790, 0.1600, 0.0147, 0.0038)$ and the values of parameters when $\mathcal{R}_{p_0} < 1$ given in Table 2 with $\beta = 0.96, q_p = 0.68$. In this scenario, $\mathcal{R}_{p_0} = 0.0051 < 1$ and hence, Model (13) has one disease-free equilibrium $T_p^\circ = (1.3747 \times 10^7, 0, 0, 0, 0)$ and it is globally asymptotically stable, which means that the disease disappears. This result is illustrated in Figure 3. Similarly to the second scenario when $\mathcal{R}_{p_0} > 1$ with $\beta = 0.96, q_p = 6.8$. We get $\mathcal{R}_{p_0} = 8.6474 > 1$. Consequently, Model (13) has a unique endemic equilibrium $T_p^* = (1.5897 \times 10^6, 8.9063 \times 10^6, 1.0502 \times 10^5, 2.9311 \times 10^6, 7.0673 \times 10^4)$. Additionally, it is globally asymptotically stable. This result is sketched in Figure 6 and illustrates the continued prevalence of the disease among the population.

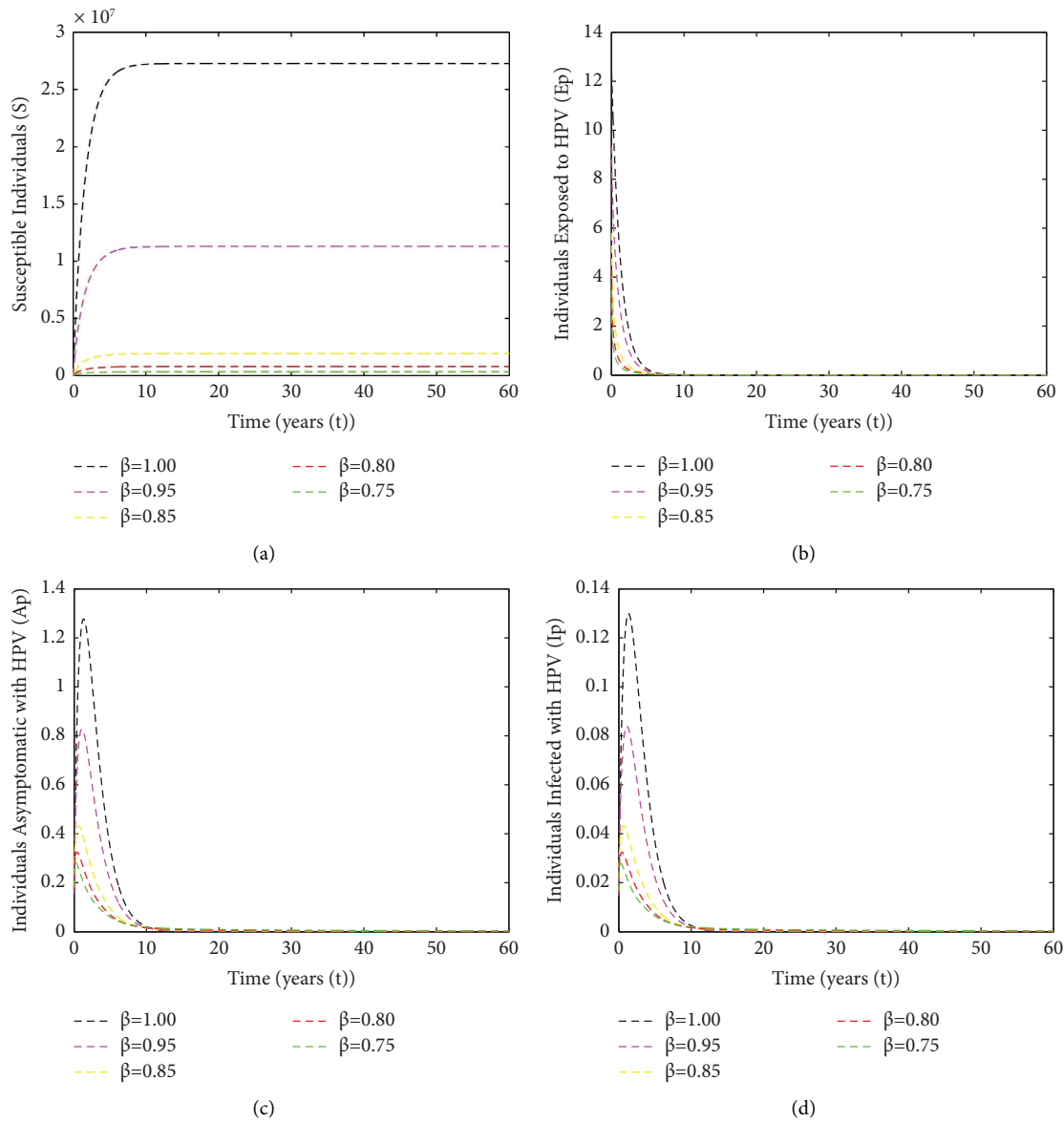
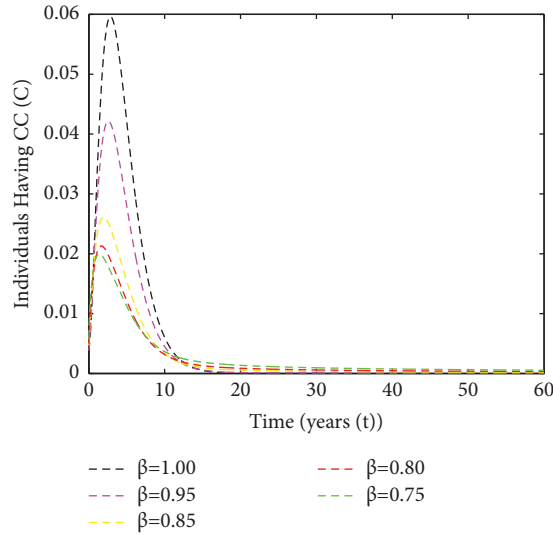
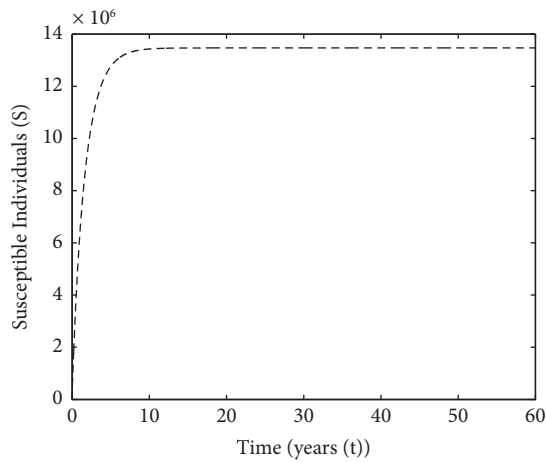


FIGURE 2: Continued.

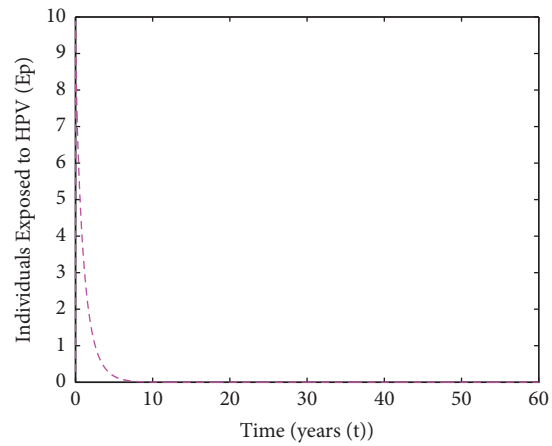


(e)

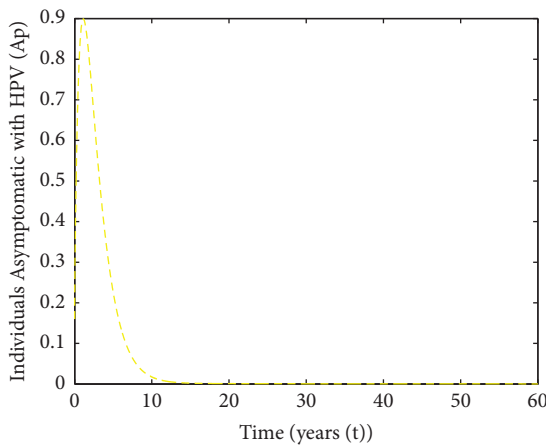
FIGURE 2: Dynamics of model (13) when $\mathcal{R}_{p_0} < 1$ applying scheme (44) at a time step size $\delta_t = 0.02$ with five different initial conditions that satisfy Theorem 23 as well as five different values of $\beta (\in 0, 1]$, and $q_p = 0.68$. All other parameters are as in Table 2 when $\mathcal{R}_{p_0} < 1$. (a) Dynamics of susceptible individuals. (b) Dynamics of individuals exposed to HPV. (c) Dynamics of individuals asymptomatic with HPV. (d) Dynamics of individuals infected with HPV. (e) Dynamics of individuals having CC.



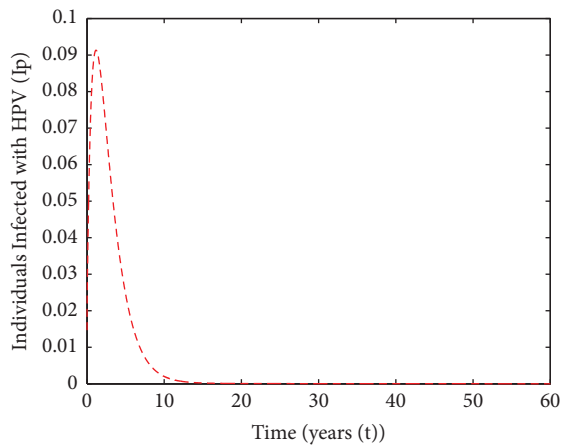
(a)



(b)



(c)



(d)

FIGURE 3: Continued.

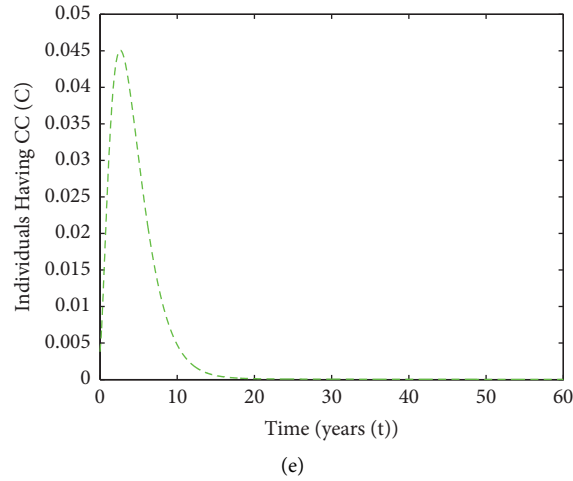


FIGURE 3: Dynamics of model (13) when $\mathcal{R}_{p_0} = 0.0051 < 1$ applying scheme (44) at a time step size $\delta_t = 0.02$ with initial condition $(S(0), E_p(0), A_p(0), I_p(0), C(0)) = (0.5425, 0.2790, 0.1600, 0.0147, 0.0038)$ and $\beta = 0.96, q_p = 0.68$. All other parameters are as in Table 2 when $\mathcal{R}_{p_0} < 1$. (a) Dynamics of susceptible individuals. (b) Dynamics of individuals exposed to HPV. (c) Dynamics of individuals asymptomatic with HPV. (d) Dynamics of individuals infected with HPV. (e) Dynamics of individuals having CC.

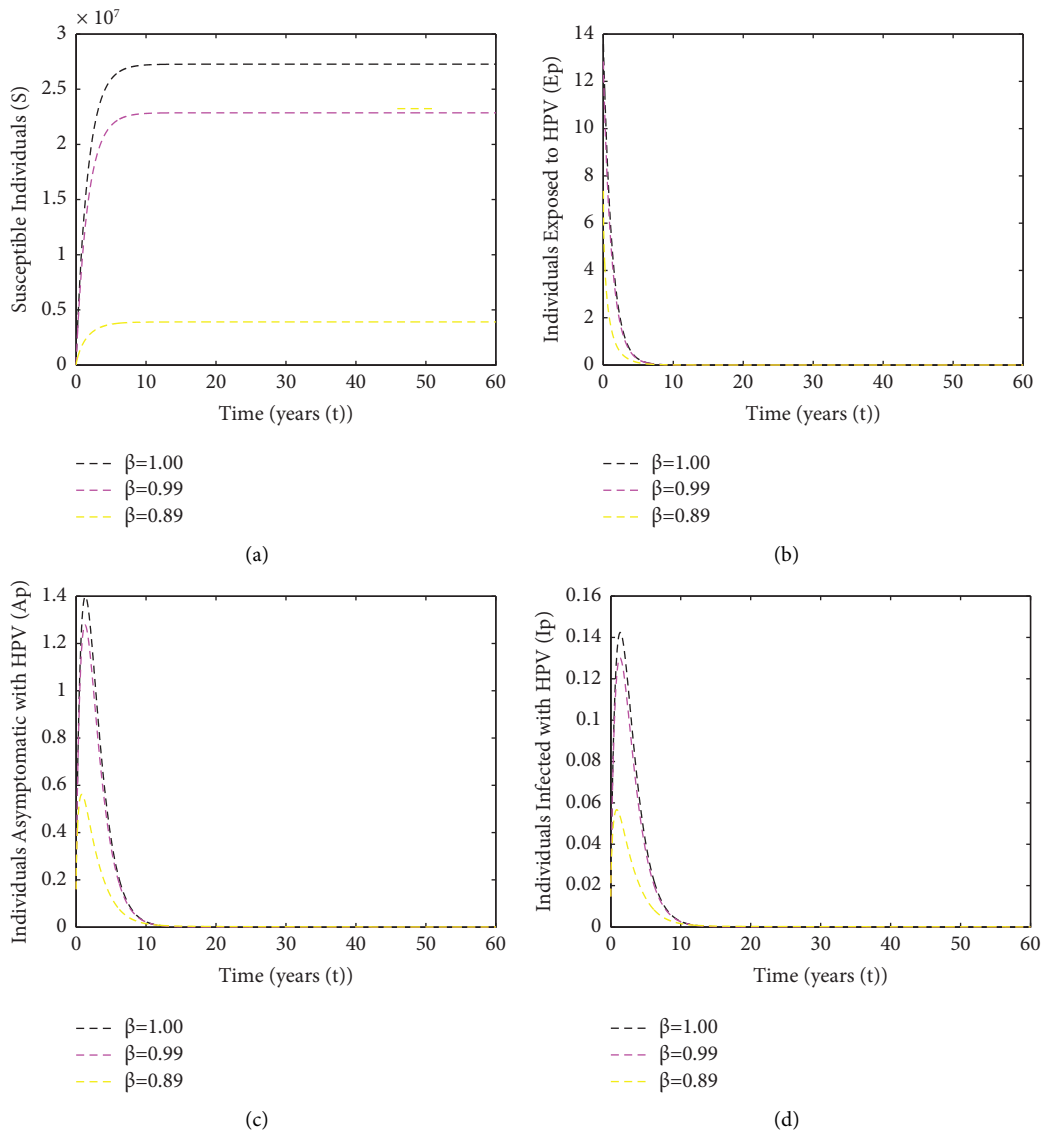


FIGURE 4: Continued.

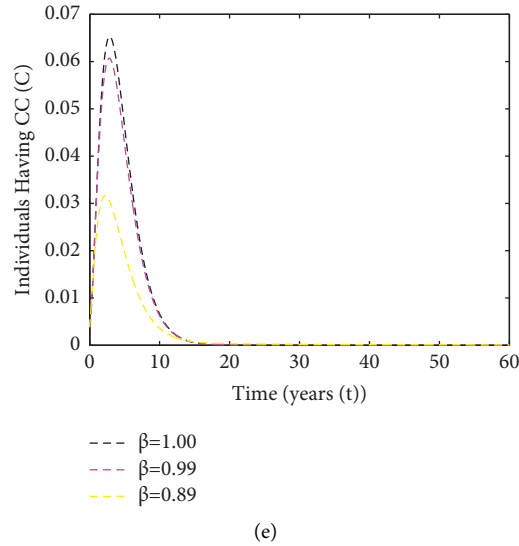


FIGURE 4: Numerical results showing a comparison between integer-order model (10) and fractional-order model (13) with $\beta = 0.99$ and 0.89 applying scheme (44) at a time step size $\delta_t = 0.02$ with initial condition $(S(0), E_p(0), A_p(0), I_p(0), C(0)) = (0.5425, 0.2790, 0.1600, 0.0147, 0.0038)$. $q_p = 0.75$ and all other parameters are as in Table 2 when $\mathcal{R}_{p_0} < 1$. (a) Dynamics of susceptible individuals. (b) Dynamics of individuals exposed to HPV. (c) Dynamics of individuals asymptomatic with HPV. (d) Dynamics of individuals infected with HPV. (e) Dynamics of individuals having CC.

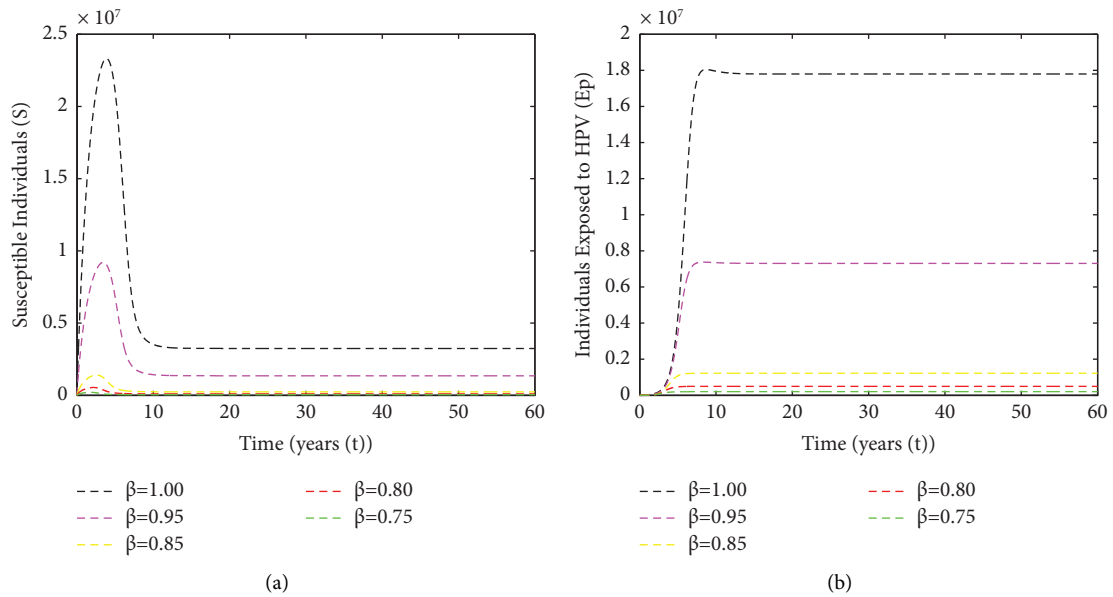


FIGURE 5: Continued.

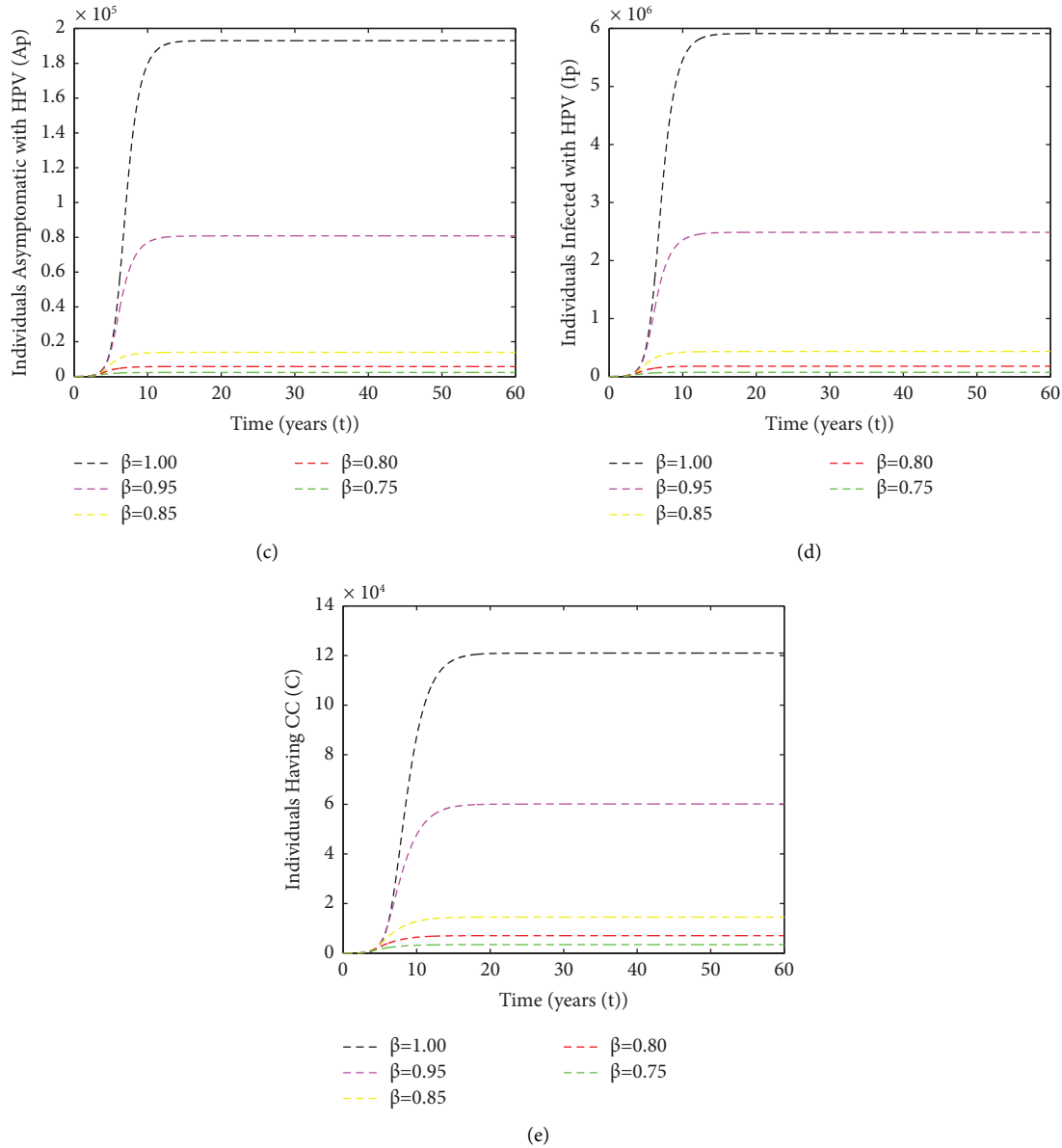


FIGURE 5: Dynamics of model (13) when $\mathcal{R}_{p_0} > 1$ applying scheme (44) at a time step size $\delta_t = 0.02$ with five different initial conditions that satisfy Theorem 23 as well as five different values of $\beta (\in 0, 1]$, and $q_p = 6.8$. All other parameters are as in Table 2 when $\mathcal{R}_{p_0} > 1$. (a) Dynamics of susceptible individuals. (b) Dynamics of individuals exposed to HPV. (c) Dynamics of individuals asymptomatic with HPV. (d) Dynamics of individuals infected with HPV. (e) Dynamics of individuals having CC.

Figures 4 and 7 provide the numerical results for the distinction between fractional and integer orders. Figures 4 and 7 demonstrate that, in comparison to classical integer-order models, differential equations with fractional-order derivatives have wealthy dynamics and more accurately depict biological systems.

Drawing from the preceding discussion and the numerical results presented in Figures 2–7, we deduce that β may be influenced by an individual’s prior experience with or understanding of the illness. Consequently, the numerical results validate that differential equations with fractional-order derivatives explain biological systems more accurately than classical integer-order models.

Depending on the values of the parameters mentioned in Table 2, Tables 3 and 4 show how q_p has an impact on decreasing and increasing \mathcal{R}_{p_0} , respectively. The prevalence of HPV-CC is influenced by the level of interpersonal contact within a community (q_p).

By analyzing these variations, we may predict more about how fractional orders affect the model’s dynamics and how crucial the parameter q_p is in influencing population dynamics. Moreover, Figures 2–7 present results that provide a basis for additional investigation and refinement of the model, which could result in the development of more potent disease control and prevention techniques.

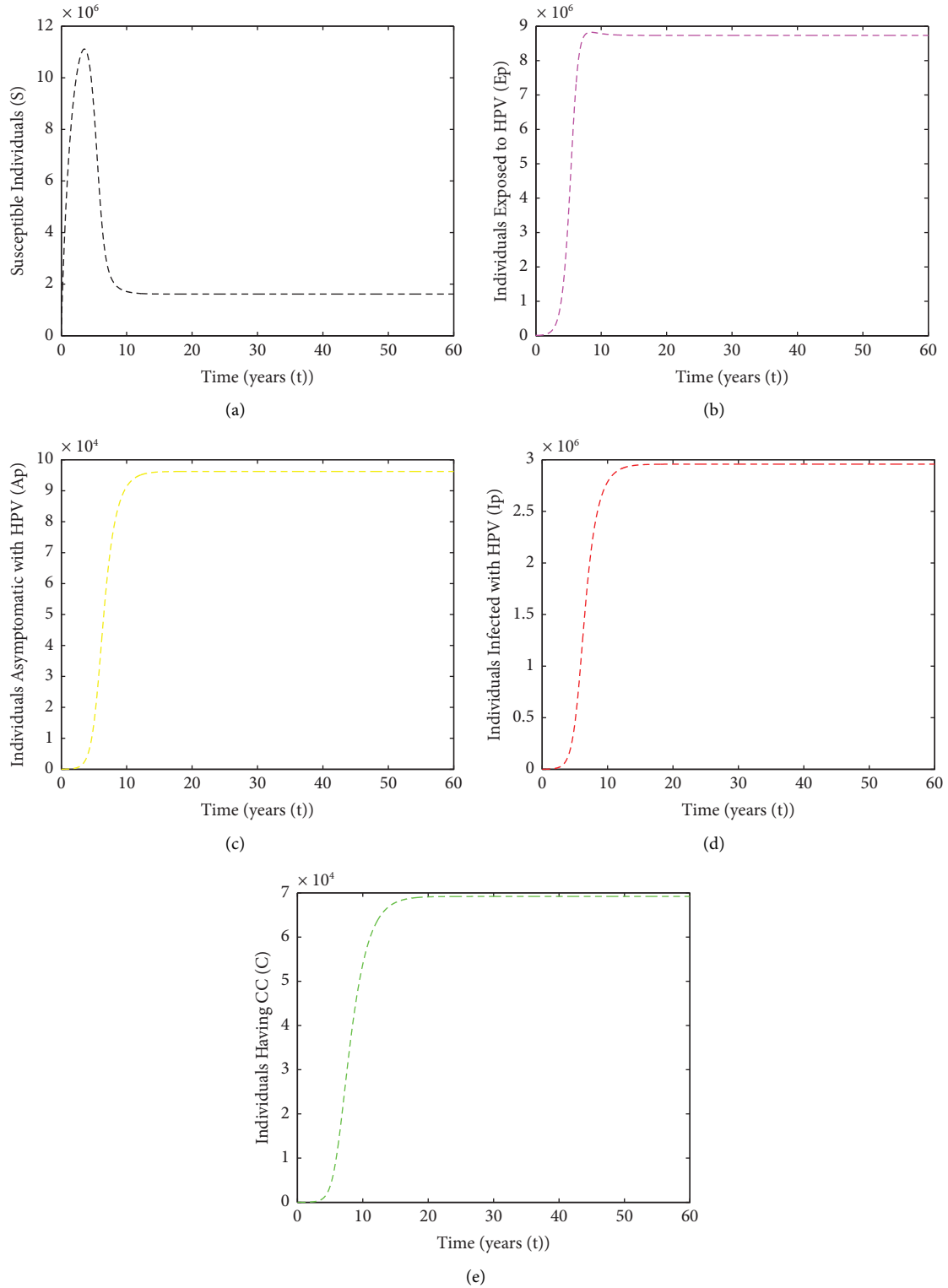


FIGURE 6: Dynamics of model (13) when $\mathcal{R}_{p_0} = 8.6474 > 1$ applying scheme (44) at a time step size $\delta_t = 0.02$ with initial condition $(S(0), E_p(0), A_p(0), I_p(0), C(0)) = (0.5425, 0.2790, 0.1600, 0.0147, 0.0038)$ and $\beta = 0.96, q_p = 6.8$. All other parameters are as in Table 2 when $\mathcal{R}_{p_0} > 1$. (a) Dynamics of susceptible individuals. (b) Dynamics of individuals exposed to HPV. (c) Dynamics of individuals asymptomatic with HPV. (d) Dynamics of individuals infected with HPV. (e) Dynamics of individuals having CC.

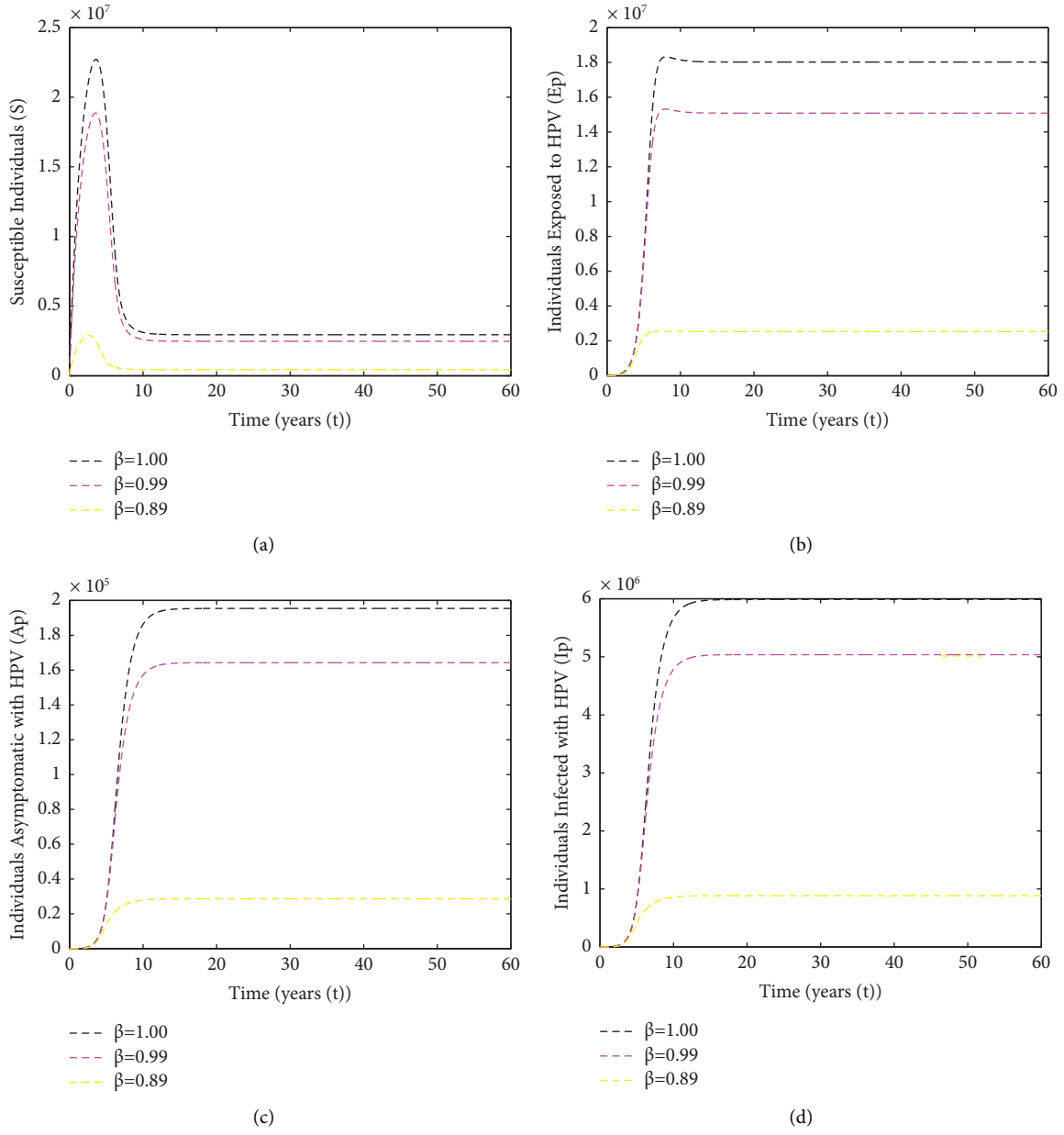


FIGURE 7: Continued.

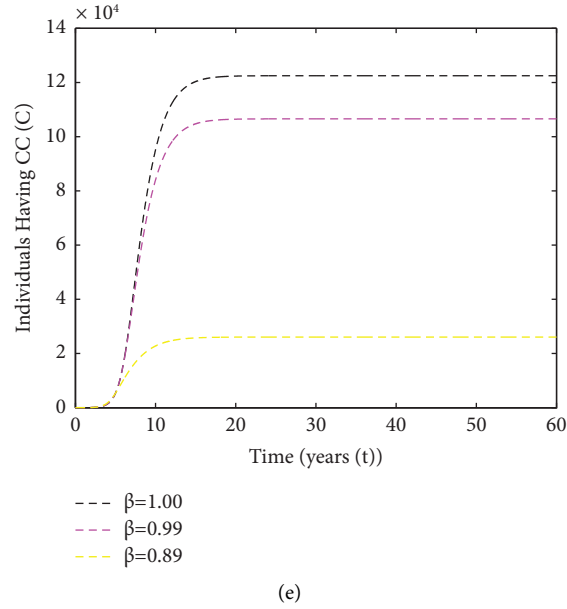


FIGURE 7: Numerical results showing a comparison between integer-order model (10) and fractional-order model (13) with $\beta = 0.99$ and 0.89 applying scheme (44) at a time step size $\delta_t = 0.02$ with initial condition $(S(0), E_p(0), A_p(0), I_p(0), C(0)) = (0.5425, 0.2790, 0.1600, 0.0147, 0.0038)$. $q_p = 7.5$ and all other parameters are as in Table 2 when $\mathcal{R}_{p_0} > 1$. (a) Dynamics of susceptible individuals. (b) Dynamics of individuals exposed to HPV. (c) Dynamics of individuals asymptomatic with HPV. (d) Dynamics of individuals infected with HPV. (e) Dynamics of individuals having CC.

TABLE 3: Impact of changing q_p on \mathcal{R}_{p_0} in the case of disease-free.

β	r_4	r_3	q	\mathcal{B}_p	q_p	\mathcal{R}_{p_0}
0.70	0.0531	0.0376	0.091	0.41	0.75	0.0129
					0.70	0.0121
					0.65	0.0112
					0.60	0.0103
					0.55	0.0095

TABLE 4: Impact of changing q_p on \mathcal{R}_{p_0} in the case of epidemic.

β	r_4	r_3	q	\mathcal{B}_p	q_p	\mathcal{R}_{p_0}
0.70	0.590	0.376	0.967	5.0	7.5	11.2018
					7.0	10.4550
					6.5	9.7083
					6.0	8.9615
					5.5	8.2147

8. Conclusion and Future Directions

In this article, we proposed a fractional-order HPV with cervical cancer (HPV-CC) model with Caputo derivative of order $\beta (\in 0, 1]$. This dynamical model was more compatible for describing biological phenomena with memory than the integer-order model. Some mathematical results related to the model are presented. The local stability of the model for $\mathcal{R}_{p_0} < 1$ and $\mathcal{R}_{p_0} > 1$ was given. The model had two equilibrium points: the disease-free point (T_p^o) and the endemic point (T_p^*). The examination of the system's local and global

stability was provided in terms of the basic reproductive number (\mathcal{R}_{p_0}). Using LaSalle invariant principle and the appropriate Lyapunov function, the analysis of global stability had been conducted. The results demonstrated that in the infection model, if $\mathcal{R}_{p_0} < 1$, then the solution converged to T_p^o , which was both locally and globally asymptotically stable. Whilst $\mathcal{R}_{p_0} > 1$, T_p^* was considered to exist. To determine how changes in parameters affect the dynamic behavior of the proposed system, simulations were constructed using a finite difference scheme with Grünwald-Letnikov discretization approach for Caputo derivative

operator. The outcomes acquired demonstrated that the finite difference method is a precise and effectual technique to obtain the numerical solution of the suggested nonlinear fractional-order HPV-CC model.

In future work, the presented model after being modified, will be integrated with HIV-AIDS; employing nonlocal and nonsingular kernel operators such as Caputo-Fabrizio. The generalized Adams-Bashforth Moulton method will be applied for the numerical simulations.

Data Availability

No data were used to support this study.

Conflicts of Interest

There authors declare that there are no conflicts of interest.

References

- [1] E. Dadi Gurmu and P. Rao Koya, "Sensitivity analysis and modeling the impact of screening on the transmission dynamics of human papilloma virus (HPV)," *American Journal of Applied Mathematics*, vol. 7, no. 3, pp. 70–79, 2019.
- [2] L. B. R. L. Bruni, L. Barrionuevo-Rosas, G. Albero et al., *Human papillomavirus and related diseases in the world*, ICO HPV Information Centre, Barcelona, Spain, 2015.
- [3] A.-S. Bergot, A. Kassianos, I. H. Frazer, and D. Mittal, "New approaches to immunotherapy for HPV associated cancers," *Cancers*, vol. 3, no. 3, pp. 3461–3495, 2011.
- [4] L. M. de S. Souza, W. M. Miller, J. A. da C. Nery, A. F. B. d Andrade, and M. D. Asensi, "A syphilis co-infection study in human papilloma virus patients attended in the sexually transmitted infection ambulatory clinic, Santa Casa de Misericórdia Hospital, Rio de Janeiro, Brazil," *Brazilian Journal of Infectious Diseases*, vol. 13, no. 3, pp. 207–209, 2009.
- [5] N. Shahzad, R. Farooq, B. Aslam, and M. Umer, "Microbicides for the Prevention of HPV, HIV-1, and HSV-2: Sexually Transmitted Viral Infections," *Fundamentals of sexually transmitted infections*, IntechOpen, London, UK, 2017.
- [6] S. de Sanjose, M. Brotons, and M. A. Pavon, "The natural history of human papillomavirus infection," *Best Practice and Research Clinical Obstetrics & Gynaecology*, vol. 47, pp. 2–13, 2018.
- [7] World Health Organization, "Global strategy to accelerate the elimination of cervical cancer as a public health problem," 2020, <https://apps.who.int/iris/bitstream/handle/10665/336583/9789240014107-eng.pdf>.
- [8] H. Sung, J. Ferlay, R. L. Siegel et al., "Global cancer statistics 2020: GLOBOCAN estimates of incidence and mortality worldwide for 36 cancers in 185 countries," *CA: A Cancer Journal for Clinicians*, vol. 71, no. 3, pp. 209–249, 2021.
- [9] P. Yadav, S. Jahan, K. Shah, O. J. Peter, and T. Abdeljawad, "Fractional-order modelling and analysis of diabetes mellitus: utilizing the Atangana-Baleanu Caputo (ABC) operator," *Alexandria Engineering Journal*, vol. 81, pp. 200–209, 2023.
- [10] R. Aris, "Mathematical modelling techniques," *Courier Corporation*, 2012.
- [11] H. T. Alemneh and A. M. Belay, "Modelling, analysis, and simulation of measles disease transmission dynamics," *Discrete Dynamics in Nature and Society*, vol. 2023, Article ID 9353540, 20 pages, 2023.
- [12] R. V. Culshaw and S. Ruan, "A delay-differential equation model of HIV infection of CD4+ T-cells," *Mathematical Biosciences*, vol. 165, no. 1, pp. 27–39, 2000.
- [13] D. Baleanu, A. K. Golmankhaneh, A. K. Golmankhaneh, and R. R. Nigmatullin, "Newtonian law with memory," *Nonlinear Dynamics*, vol. 60, no. 1-2, pp. 81–86, 2010.
- [14] S. Qureshi, "Real life application of Caputo fractional derivative for measles epidemiological autonomous dynamical system," *Chaos, Solitons & Fractals*, vol. 134, 2020.
- [15] F. Özköse and M. Yavuz, "Investigation of interactions between COVID-19 and diabetes with hereditary traits using real data: a case study in Turkey," *Computers in Biology and Medicine*, vol. 141, 2022.
- [16] C. T. Deressa, S. Etemad, and S. Rezapour, "On a new four-dimensional model of memristor-based chaotic circuit in the context of nonsingular Atangana–Baleanu–Caputo operators," *Advances in Difference Equations*, vol. 2021, pp. 444–524, 2021.
- [17] K. M. Owolabi, *Abdon Atangana. Numerical methods for fractional differentiation*, vol. 54, Springer, Singapore, 2019.
- [18] C. T. Deressa and G. F. Duressa, "Analysis of Atangana–Baleanu fractional-order SEAIR epidemic model with optimal control," *Advances in Difference Equations*, vol. 2021, pp. 174–225, 2021.
- [19] S. Paul, A. Mahata, S. Mukherjee, P. C. Mali, and B. Roy, "Dynamical behavior of fractional order SEIR epidemic model with multiple time delays and its stability analysis," *Examples and Counterexamples*, vol. 4, 2023.
- [20] H. Jahanshahi, J. M. Munoz-Pacheco, S. Bekiros, and N. D. Alotaibi, "A fractional-order SIRD model with time-dependent memory indexes for encompassing the multifractional characteristics of the COVID-19," *Chaos, Solitons and Fractals*, vol. 143, 2021.
- [21] P. A. Naik, J. Zu, and K. M. Owolabi, "Global dynamics of a fractional order model for the transmission of HIV epidemic with optimal control," *Chaos, Solitons and Fractals*, vol. 138, 2020.
- [22] Yu-M. Chu, M. F. Khan, S. Ullah, S. A. A. Shah, M. Farooq, and M. bin Mamat, "Mathematical assessment of a fractional-order vector–host disease model with the Caputo–Fabrizio derivative," *Mathematical Methods in the Applied Sciences*, vol. 46, no. 1, pp. 232–247, 2023.
- [23] K. R. Cheneke, "Fractional derivative model for analysis of HIV and malaria transmission dynamics," *Discrete Dynamics in Nature and Society*, vol. 2023, Article ID 5894459, 17 pages, 2023.
- [24] K. M. Owolabi and E. Pindza, "A nonlinear epidemic model for tuberculosis with Caputo operator and fixed point theory," *Healthcare Analytics*, vol. 2, 2022.
- [25] B. Fernández-Carreón, J. M. Munoz-Pacheco, E. Zambrano-Serrano, and O. G. Félix-Beltrán, "Analysis of a fractional-order glucose-insulin biological system with time delay," *Chaos Theory and Applications*, vol. 4, no. 1, pp. 10–18, 2022.
- [26] S. Moualkia, "Mathematical analysis of new variant Omicron model driven by Lévy noise and with variable-order fractional derivatives," *Chaos, Solitons and Fractals*, vol. 167, 2023.
- [27] A. Atangana, A. Akgül, and K. M. Owolabi, "Analysis of fractal fractional differential equations," *Alexandria Engineering Journal*, vol. 59, no. 3, pp. 1117–1134, 2020.
- [28] K. Zhang, X. W. Wang, H. Liu et al., "Mathematical analysis of a human papillomavirus transmission model with vaccination and screening," *Mathematical Biosciences and Engineering*, vol. 17, no. 5, pp. 5449–5476, 2020.

- [29] S. Chakraborty, J. Pal, S. Chowdhury, and P. K. Roy, "The impact of vaccination to control human papillomavirus dynamics," in *Industrial Mathematics and Complex Systems*, pp. 237–247, Springer, Singapore, 2017.
- [30] Z. Ul A. Zafar, M. T. Hussain, M. Inc et al., "Fractional-order dynamics of human papillomavirus," *Results in Physics*, vol. 34, 2022.
- [31] F. Saldaña, J. A. Camacho-Gutiérrez, G. Villavicencio-Pulido, and J. X. Velasco-Hernández, "Modeling the transmission dynamics and vaccination strategies for human papillomavirus infection: an optimal control approach," *Applied Mathematical Modelling*, vol. 112, pp. 767–785, 2022.
- [32] V. V. Akimenko and F. Adi-Kusumo, "Stability analysis of an age-structured model of cervical cancer cells and HPV dynamics," *Mathematical Biosciences and Engineering*, vol. 18, no. 5, pp. 6155–6177, 2021.
- [33] K. Allali, "Stability analysis and optimal control of HPV infection model with early-stage cervical cancer," *Biosystems*, vol. 199, 2021.
- [34] Z. Chazuka, G. M. Moremedi, and E. Rapoo, "In-host dynamics of the human papillomavirus (HPV) in the presence of immune response," in *International Symposium on Mathematical and Computational Biology*, pp. 79–97, Springer, Berlin, Germany, 2020.
- [35] E. R. Sari, F. Adi-Kusumo, and L. Aryati, "Mathematical analysis of a SIPC age-structured model of cervical cancer," *Mathematical Biosciences and Engineering*, vol. 19, no. 6, pp. 6013–6039, 2022.
- [36] M. Goshu and A. Abebe, "Mathematical modelling of cervical cancer vaccination and treatment effectiveness," 2022.
- [37] A. Omame, D. Okuonghae, U. E. Nwafor, and B. U. Odionyenma, "A co-infection model for HPV and syphilis with optimal control and cost-effectiveness analysis," *International Journal of Biomathematics*, vol. 14, no. 7, 2021.
- [38] U. K. Nwajeri, A. B. Panle, A. Omame, M. C. Obi, and C. P. Onyenegecha, "On the fractional order model for HPV and Syphilis using non-singular kernel," *Results in Physics*, vol. 37, 2022.
- [39] A. Omame, C. U. Nnanna, and S. C. Inyama, "Optimal control and cost-effectiveness analysis of an HPV-Chlamydia trachomatis co-infection model," *Acta Biotheoretica*, vol. 69, no. 3, pp. 185–223, 2021.
- [40] U. K. Nwajeri, A. Omame, and C. P. Onyenegecha, "Analysis of a fractional order model for HPV and CT co-infection," *Results in Physics*, vol. 28, 2021.
- [41] E. D. Gurmu, B. K. Bole, and P. Rao Koya, "Analysis of optimal control strategy on transmission dynamics of HPV-HSV-II coinfection model," *Journal of applied research on industrial engineering*, vol. 9, no. 3, pp. 231–248, 2022.
- [42] E. D. Gurmu, B. K. Bole, and P. R. Koya, "Mathematical model for co-infection of HPV with cervical cancer and HIV with AIDS diseases," *International journal of scientific research in mathematical and statistical sciences*, vol. 7, no. 2, 2020.
- [43] W.. Lin, "Global existence theory and chaos control of fractional differential equations," *Journal of Mathematical Analysis and Applications*, vol. 332, no. 1, pp. 709–726, 2007.
- [44] Z. M. Odibat and N. T. Shawagfeh, "Generalized Taylor's formula," *Applied Mathematics and Computation*, vol. 186, no. 1, pp. 286–293, 2007.
- [45] C. M. Pinto and A. R. Carvalho, "A latency fractional order model for HIV dynamics," *Journal of Computational and Applied Mathematics*, vol. 312, pp. 240–256, 2017.
- [46] P. Van den Driessche and J. Watmough, "Reproduction numbers and sub-threshold endemic equilibria for compartmental models of disease transmission," *Mathematical Biosciences*, vol. 180, no. 1-2, pp. 29–48, 2002.
- [47] C.. Vargas-De-León, "Volterra-type Lyapunov functions for fractional-order epidemic systems," *Communications in Nonlinear Science and Numerical Simulation*, vol. 24, no. 1-3, pp. 75–85, 2015.
- [48] La Salle and P. Joseph, *An invariance principle in the theory of stability*, Brown University, Providence, RI, USA, 1966.
- [49] R. Scherer, S. L. Kalla, Y. Tang, and J. Huang, "The Grünwald–Letnikov method for fractional differential equations," *Computers and Mathematics with Applications*, vol. 62, no. 3, pp. 902–917, 2011.
- [50] S. Pooseh, R. Almeida, and D. F. M. Torres, "Approximation of fractional integrals by means of derivatives," *Computers and Mathematics with Applications*, vol. 64, no. 10, pp. 3090–3100, 2012.
- [51] G. González-Parra, A. J. Arenas, and B. M. Chen-Charpentier, "A fractional order epidemic model for the simulation of outbreaks of influenza A (H1N1)," *Mathematical Methods in the Applied Sciences*, vol. 37, no. 15, pp. 2218–2226, 2014.